ISSN: 2454-1311

International Journal of Advanced Engineering, Management and Science

Journal CrossRef DOI: 10.22161/ijaems

(IJAEMS)

An Open Access Peer-Reviewed International Journal

Vol-10, Issue- 2 | Feb 2024

Issue DOI: 10.22161/ijaems.102

INFOGAIN PUBLICATION

https://www.ijaems.com/ | ijaems.editor@gmail.com

International Journal of Advanced Engineering, Management and Science (IJAEMS)

(ISSN: 2454-1311)

DOI: 10.22161/ijaems

Vol-10, Issue-2

February, 2024

Publisher

Infogain Publication

Email: ijaems.editor@gmail.com ; editor@ijaems.com

Web: www.ijaems.com

Editorial Board/ Reviewer Board

Vol-10, Issue-2, February, 2024

(10.22161/ijaems.102)

Sr No.	Title with Article detail
1	***A Review of the Buying behaviour of the Millennials in India*** *Megha Sethi* ***DOI: 10.22161/ijaems.102.1*** *Page No: 01-06*
2	***Green synthesis of iron-organic framework Fe-BTC using direct ultrasound to remove methylene blue dye*** *Nam Ho Phung Khac* ***DOI: 10.22161/ijaems.102.2*** *Page No: 07-13*
3	***Effect of Replacement Layers on Bearing Capacity of Silty Clay Layer*** *Mohamed A. Jpr, Alnos A. Easa, Elsayed A. El-Kasaby* ***DOI: 10.22161/ijaems.102.3*** *Page No: 14-22*
4	***Study the effect of Industrial Dairy, Textile, Leather and Paper Waste Water on the Engineering and Geotechnical Properties of Fine-Grained Soil*** *Elsayed A. El Kasaby, Alnos A. Eissa, Alaa F. Essa, Eman M. Hawari* ***DOI: 10.22161/ijaems.102.4*** *Page No: 23-39*

INFOGAIN PUBLICATION

International Journal of Advanced Engineering, Management and Science (IJAEMS)
Peer-Reviewed Journal
ISSN: 2454-1311 | Vol-10, Issue-2; Feb, 2024
Journal Home Page: https://ijaems.com/
DOI: https://dx.doi.org/10.22161/ijaems.102.1

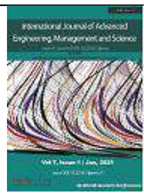

A Review of the Buying behaviour of the Millennials in India

Megha Sethi

Research Scholar, Department of Commerce, University of Delhi, India

Received: 09 Dec 2023; Received in revised form: 16 Jan 2024; Accepted: 26 Jan 2024; Available online: 06 Feb 2024

***Abstract*— *Consumer shopping behavior has undergone a profound and permanent transformation due to the evolution of the Internet, social networking, and the introduction of mobile devices. The current booming segments that are being lured by the companies are the Millennials and Generation Z because of which the global market is flourishing. They are considered as the most loyal consumers because of their good reach and connectivity. This study focuses on the buying behaviour of these millennials.*

Keywords*— consumer behaviour, Generation X & Y, millennials, technology.

I. INTRODUCTION

The study discusses the impact of generational differences on consumer behavior, emphasizing the evolving landscape shaped by various factors such as technological advancements, societal changes, and economic shifts. The focus is particularly on Millennials, born between 1980 and 2000, who are identified as a unique and influential consumer group.

Generational cohorts, as proposed by Howe and Strauss, are seen as aggregates of individuals with shared experiences and beliefs due to the historical events occurring during their formative years. The study emphasizes the importance of understanding these generational dynamics in the realm of consumer behavior, as they influence preferences, attitudes, and purchasing patterns.

The rise of Millennials is highlighted, being the largest and best-educated generation globally. The text points out their unique characteristics and the potential they present for businesses. However, it also notes the challenges faced by Millennials in developed countries, such as unemployment, housing issues, and student debt burdens.

The impact of technology on Millennials is a central theme, emphasizing their digital engagement, particularly with mobile devices. Millennials' dependence on smartphones for various activities, including shopping, socializing, and media consumption, is explored. Their interactions with brands on social media are characterized by a quest for deals, coupons, and specialized information rather than brand loyalty.

Moreover, the text underscores the importance of analyzing Millennials' digital behavior for brands to succeed in influencing this demographic. It highlights Millennials' preference for customization, and personalization, and their inclination to be influenced by celebrities, vloggers, and peers. Traditional advertising methods are considered less effective due to changing lifestyle patterns.

Additionally, the discussion touches on the global distribution of Millennials, with significant populations in countries like India and China. The text suggests that while Millennials in developing countries may have high potential, their limited purchasing power affects their economic impact.

In conclusion, the summary captures the essence of the text, emphasizing the influence of generational cohorts, particularly Millennials, on consumer behavior. The impact of technology, the challenges faced by Millennials, and their unique preferences in the market are key themes explored in the context of global consumer dynamics.

II. LITERATURE REVIEW

Each generation is endowed with unique characteristics shaped by Earth's events, influencing and, in turn, impacting the world. The global landscape is on the brink of being governed by a new generation, demanding our preparation. News has become as accessible as a mobile phone, necessitating a re-evaluation of ancient norms and approaches to align with contemporary needs.

From a pessimistic viewpoint, this emerging generation is often criticized as lazy, irresponsible, impatient, apathetic, vain, disrespectful, and wasteful in the millennium context. However, an optimistic perspective portrays them as open-minded, social, innovative, energetic, ambitious, confident, motivated, and intelligent. A common thread among them is their affinity for consumerism.

Consumer behaviour is the primary field and source for Customer Relationship Management (CRM) programs. Understanding the adjustments in consumption patterns through generational strategies is crucial. Generational lifestyles and cultural attitudes influence purchasing decisions, with demographic variables such as income, education, and gender playing a significant role.

Different generations face varying personal, financial, technological, cultural, and life-related factors. Consumer motivation and buying commitment are often age-dependent, necessitating a nuanced understanding of generational cohorts. These cohorts, individuals born during a specific era with mutually consistent lives, play a pivotal role in market segmentation. Cohort marketing has become an essential tool in understanding economies, as individuals within cohorts share similar beliefs and unique experiences influencing their preferences and purchasing behaviour.

While the purchasing power of baby boomers has historically driven the economy, this group is aging, and a broader sector now receives a substantial portion of consumer spending. The Millennial community, or Generation Y, has emerged as a significant force in the market, surpassing Generation X and even outpacing baby boomers threefold. Studying the factors influencing Millennials, such as their future spending strength, trend-setting abilities, adoption of new products, and customization preferences, has become a crucial aspect of consumer studies.

Macro-level cultural, political, and economic developments during a cohort's pre-adult years contribute to the formation of a generational identity, characterized by distinct values, opinions, aspirations, and behaviours. These ideals persist throughout a family's life, providing a constant framework for understanding generational dynamics.

(Howe and Strauss) introduced the generational hypothesis in their book "Generations: The Story of America's Future, 1584-2069." They propose that a social generation comprises individuals born within a roughly 20-year span, sharing common cultural, social, political, and historical experiences throughout childhood, growth, and adulthood, leading to shared beliefs and actions. The term "economic generation," defined by **(Strauss and Howe)**, represents an average duration of about 20 years, covering stages from infancy to old age. Specific generations, from their initial to final years, are identified based on certain criteria within this timeframe.

Members of a generation, positioned at a specific age in history, undergo similar life cycles, participating in crucial historical developments and social trends. The enduring influence of leaders within a group during their formative years contributes to shared beliefs and behaviors, fostering a collective sense of membership within that generation. Strauss and Howe's theory asserts that historical ages are shaped by various generations living in different periods.

Their research, outlined in "Generations," is recognized as pioneering work that comprehensively understands the history of generational trends, strengthens the influence of advertising across generations, revolutionizes modern thought shaped by generational differences, and aids in comprehending non-demographically established decades. The generation succeeding the Baby Boomers is termed the 13th generation, roughly equivalent to Generation X, with those born after 1982 being recognized as part of the Millennial Generation (Generation Y).

In a subsequent work, (Howe and Strauss) delve into the historical phases influencing Generation X and Generation Y, providing insights into America's initial encounters with destiny. **(Erickson)** contrasts the generations of India with the United States, elucidating how distinct social, political, and economic circumstances have shaped different generations in India during various periods.

(Bachler) contributed to a journal with an essay focusing on targeting Generation X and Generation Y in America. Throughout the essay, Bachler discussed various characteristics of both generations, including their preferences, dislikes, and favourite places. The article aimed to provide insights for advertisers to tailor their strategies. It compared different marketing tools such as the internet, radio, publications, and direct mail for effectively reaching these target groups.

(Richard Sayers) addressed the growing challenge for businesses and public sector organizations to attract and retain talented workers, especially among the younger and highly qualified workforce. Workplace readiness's importance and generational changes' impact on organizations were explored. The survey covered countries in East Asia, South-East Asia, and the United Kingdom, including China, India, Indonesia, Pakistan, Philippines, Singapore, Thailand, and Australia. The paper argued that understanding generational changes and contributing to professional development is vital for attracting and retaining talent in future academic libraries.

(La Toya M Robbins) conducted research on leadership growth in the Platteville area for both generations in comparison to baby boomers. The article delves into how traditional and modern methodologies and ideas can be integrated to cultivate effective leaders.

(Tolbiz) analyzed generational differences among American employees in the workplace. The research examined various factors, including attitudes toward the job, employer loyalty, respect for authority, learning and training preferences, and the inclination for a favourable work/life balance. The study identified several similarities and distinctions among the surveyed generations, including traditional, baby boomers, Generation X, and Generation Y.

(Susana Fernandez) compared the work-related attitudes of Silicon Valley workers from Generation X and Generation Y. The research investigated potential differences between generations and genders concerning three job-related convictions: employment, teamwork, and career development. The findings indicated that Generation Y exhibits a greater interest in work compared to Generation X, and men tend to be more engaged and satisfied in their job conversations than women.

(Gayle Elizabeth Ruddick) examined the workforce dynamics of traditionalists, baby boomers, Generation X, and Generation Y. The research highlighted diverse interactions, workplace values, and requirements across the four generations. The study revealed that Generation Y seeks guidance and consultation, valuing independence while also desiring recognition and direction. Key findings addressed ideal and unacceptable work qualities, effective and ineffective interaction, and perceptions of leadership communication.

(Marketingcharts.com) explored how Generation X and Generation Y contribute to economic recovery. The study identified top spending categories for the younger generation, including clothes, travel/holidays, footwear, and theatre-based films. **(Sylvia J. Jaros)** examined intergenerational tensions among female employees, focusing on the forms and differences of interaction among different generations of women.

(Mahalakshmi and Dr. K. Jawahar Rani) investigated the factors influencing the adoption and use of smartphones in Chennai for Generations X and Y. The study concluded that economic, demographic, cultural, and technological factors shape the actions of Generation X and Y in adopting and using mobile phones. The research also highlighted how both generations perceive mobile phones as status symbols that reflect their social standing and power.

The research paper by **(Kaylene C. Williams and Robert A.)** emphasized the differences in buying behaviour, perceptions, perspectives, family backgrounds, attitudes, beliefs, and demographics across generations. The study covered six generations, including pre-depression, depression, baby boomers, Generation X, Generation Y, and Generation Z. The paper underscored the importance of understanding each generation's characteristics and behaviors for effective marketing strategies, particularly in terms of segmentation, products, services, and communication.

(Ventura Institute) issued a report indicating that various companies are tailoring their strategies to target customers across different generations, including Baby Boomers, Generation X, Generation Y, and the emerging Generation Z in the United Kingdom. The study also explores how Generations X and Y can contribute as an active workforce.

(Lai Man, Stella), compared Chinese Generation X and Y females, focusing on their preferences for luxury brands and values associated with luxury. The research examined customer preferences, service habits, and actual brand purchases. Generation Y exhibited differences from its predecessor, Generation X, particularly in attitudes and values related to luxury brands. This resulted in millennials being more eligible and willing to purchase luxury products.

(Stacy Phillips) analyzed the interaction patterns, affirmation, and de-confirmation behaviors of female workers from Generation X and Generation Y, studying their impact on communication dynamics. The research concluded that there are differences in the interaction behaviour of women employees between Generation X and Generation Y.

The study conducted by the **(Talent Management Team)** in New York investigated Traditionalists, Baby Boomers, Generation X, Generation Y, and Generation Z, working together. The conclusion emphasized that businesses prepared to bridge the gap between traditionalists and Generations X and Y would thrive, attracting, retaining, and engaging employees from these generations with the upcoming demographic shift.

(Karen Ritchie) discussed Generation X marketing in a paper, highlighting how the buying behaviour of Generation X consumers is influenced by factors such as separation, diversity, and rising incomes. The purchase decisions of Generation X are impacted by family and friends, and the generation tends to avoid advertising and insincere marketing. The paper also notes the technological advancements of this generation, emphasizing the importance of the Internet. The author further addresses the influential role of Generation X in shaping the choices of friends and family.

(Jonathan Penny) delved into various payment services and options for Generation Y in his article, highlighting the increasing use of online payments and the role of the internet in shaping Generation Y's lifestyle. **(Enrique J. Fernandez)** documented the customer preferences and activities of Generation Y teens in his dissertation, analyzing their decision-making processes in purchasing goods, and considering influences from family, peers, celebrities, and information sources.

(Greg Maloney) explored the habits and shopping patterns of Generation Y consumers in his report, initially outlining the demographic, characteristics, and psychographic traits of Generation Y. The writer then delved into Generation Y's buying habits, noting their political and eco-friendly inclinations, preferences for disposable products, aversion to correctable items, and attraction to luxury shops and labels. Maloney discussed the implications of these traits for retailers and mall owners, emphasizing the need for adaptable, cross-cutting strategies sensitive to ongoing changes in retail.

(Roy Farris, Frank Chong, and Darlene Danning) analyzed Generation Y's buying habits, emphasizing the significant impact of the Internet and technology on this generation in America. The authors foresee Generation Y having a substantial economic influence.

(Alan J. Bush, Craig A. Martin, and Victoria D. Bush) explored the impact of sports stars and athletic icons on behavioural expectations in Generation Y. The study concluded that athlete role models play a significant role in spreading positive sentiments about a product or brand and fostering brand loyalty among Generation Y consumers.

(Bernard Salt) produced a consultant report for KPMG addressing the needs and expectations of Generation Y customers and employees. **(Megan E. Lodes)** conducted a preliminary study on brand loyalty, customer satisfaction, and the influences on buying patterns of Generation Y (millennial) consumers in New York. The study concluded that there were no brand loyalties, no gender differences in brand loyalty, and that economic recessions did not significantly impact buying behaviour.

(Riza Casidy) conducted a study investigating the correlation between the characteristic traits of Generation Y users, their tolerance for style, and their sensitivity to the prestige of fashion brands. The research revealed numerous personality traits significantly linked to the perception of style and prestige. It was concluded that style consciousness plays a mediating role in the relationship between personality traits and sensitivity to reputation. The study also found that personality characteristics play a crucial role in influencing individuals' attitudes towards prestigious fashion brands.

(Nicolas Maria) authored a Luxe Avenue article analyzing luxury brands among Generation Y consumers in America. The conclusion highlighted the features of Generation Y consumers, emphasizing social pressures, analysis, and a lack of engagement that drive them to purchase high-quality, well-known designer products at lower prices. **(Dr. Parul Saxena and Mr. Rajiv Jain)** published a paper on the strengths, principles, and professional expectations of Indian Generation Y. The researchers concluded that Y professionals prioritize brand identity and skills, seeking empathic bosses, good job performance, ethical business practices, and a competitive salary. Generation Y values work and social success, with a strong work ethic and quick adaptability being considered valuable attributes.

(Monika Rahulan et al.) applied the concept of generational cohorts to compare the purchasing behaviour of Generation Y cohorts with that of baby boomers, focusing on sports compression. The study aimed to understand consumer behaviour regarding factors such as comfort, performance, technological features, and brand marketing methods. The conclusion highlighted that Baby Boomers paid more attention to value factors and fashion comfort, while Generation Y discussions centered more on the aesthetic appeal of clothing and technical information on packaging and labels.

(Anders Parment) examined the purchasing behaviour and buying preferences for food, clothing, and vehicles among Swedish Generation Y. It was hypothesized that the beliefs, behaviors, and desires of Generation Y significantly affect their buying patterns. The study found that Generation Y customers are highly demanding, seeking personal attention and purchasing products that align with their lifestyle.

(Dawn B. Valentine and Thomas L. Powers) discussed the online consumer search and purchase habits of Generation Y, including product types searched and bought on the internet, product type information, reasons for not buying online, and reasons for returning goods purchased online.

(Shelja Jose Kuruvilla and Nishank Joshi) researched demographics, psychographics, shopping mall purchases, and store sponsorship routes in India. The study, involving eight cities in India, revealed that heavy shoppers significantly differed from others across various geographic, social, behavioural, shopping, and orientation variables in central India.

(Robin Pentecost and Lynda Andrews) explored the implications of fashion transactions in generational groups, ages, and fashion enthusiasts. The results indicated that gender and clothing enthusiasm significantly influenced weekly and monthly spending, with women exhibiting higher frequency, varied annual expenses, and a preference for style-related purchases. Generation Y reported higher frequency, a penchant for fashion, distinct behaviors, and energetic transactions.

III. CONCLUSION

The exploration of Millennials is of significant interest to business researchers and marketing sectors, particularly for products aiming to remain competitive in the market. This is primarily due to their widespread global population coverage and their ability to reshape purchasing patterns, challenging traditional vendors with their distinct consumption habits. A substantial portion of their purchases occurs online, prompting sellers to seek effective means of engaging with them, monitoring their behaviors, and offering products and services that align with their evolving preferences, irrespective of scale. Positive and meaningful experiences in navigating online platforms significantly influence attitudes toward the internet, subsequently impacting the inclination to make purchases. Therefore, ensuring consumers have satisfactory experiences is crucial, as favourable interactions contribute to a positive predisposition toward purchasing a product.

Millennials represent the world's second-largest population, presenting both challenges and opportunities. While currently in their college or bachelor's student phase, they are poised to dominate the workforce in the coming years. Despite some scepticism and unease among current executives, Millennials are already exerting influence on industries, not just through their purchasing power but also by shaping the buying decisions of their relatives. To effectively engage with this demographic, it is crucial for organizations and retailers to understand their perceptions, behaviors, decision-making models, and actions.

Millennials actively seek connections but value trustworthiness, emphasizing the need for a nuanced approach to engage with their complex characteristics. Rather than attempting to assimilate into their generation, establishing connections within their personal networks is key. Building trust within these networks allows organizations and retailers to influence Millennials' behavior based on research outcomes. By positioning themselves as trusted sources within Millennials' social circles, businesses can navigate the unique dynamics of this demographic.

REFERENCES

[1] Howe N, Strauss W (1991) Generations: The History of America's Future, 1584 to 2069. New York: William Morrow & Company.

[2] Strauss-Howe generational theory (2011) Wikipedia, the free encyclopedia. Retrieved June 17 2011.

[3] Erickson T (2011) Generational Differences Between India and the U.S.

[4] Bachler C (2008) How to Market to Gen X and Gen Y. Home Business® Magazine.

[5] Sayers R (2008) The Right Staff from X to Y: Generational change and professional development in future academic libraries. Australia: CAVAL Collaborative Solutions.

[6] Robbins LM (2008) Bridging the Gap in Leadership Development within Generation X and Y. University of Wisconsin- Platteville.

[7] Tolbize A (2008) Generational differences in the workplace. Research and Training Centre on Community Living. Minnesota: University of Minnesota.

[8] Fernandez S (2009) Comparing Generation X to Generation Y on work-related beliefs. San Jose State University.

[9] Ruddick GE (2009) Intergenerational Leadership Communication m the Workplace. Graduate School of Clemson University.

[10] Marketingcharts.com (2010) Splurges by Gen X, Gen Y Help Boost Economic Recovery.

[11] Jaros SJA (2010) Comparative Analysis of Intergenerational Conflict Between Women in the Workplace. Seton Hall University.

[12] Mahalakshmi S Rani J (2010) Gen X And Y Go Mobile - Exploring The Factors Affecting Their Adoption And Usage. International Journal of Enterprise and Innovation Management Studies (IJEIMS), 1: 45-52.

[13] Williams K, Page R (2010) Marketing to the Generations. Journal of Behavioral Studies in Business, 1-18.

[14] Ventura (2011) Which customer generation gets your attention? UK: Ventura.

[15] So Lai Man S (2011) Luxury Generation Gap: A Comparison between Generation X and Y. Cambridge Business & Economics Conference, p-16.

[16] Phillips S (2011) X and Y: The impact of the gap. School of Professional S111dies Faculty in Communication and Leadership Studies. Gonzaga University School of Professional Studies.

[17] TalentManagement_Team (2013) Designing Recruitment, Selection & Talent Management Model tailored to meet UNJSPF's Business Development Needs. New York: United Nations Joint Staff Pension Fund.

[18] Ritchie K (1995) Marketing to the Generation X. 17: 34-39. 27. Penny J (2001) The payments revolution: The growth of person-to-person and 'Generation Y' payments services. Journal of Financial Services Marketing, 6: 190-201.

[19] Fernandez EJ (2002) The consumer attitudes and behavioural patterns of Generation Y in Puerto Rico picture of Puerto Rican teenage consumers. Dissertation.

[20] Maloney G (2002) Gen Y and the Future of Mall Retailing. Chicago, Illinois, America.

[21] Farris R, Chong F, Danning D (2002) Generation Y: Purchasing Power and Implication For Marketing. Academy of Marketing Studies Journal, 11.

[22] Bush A, Martin C, Bush V (2004) Sports Celebrity Influence on the Behavioral Intentions of Generation Y Journal of Advertising Research, 44: 108-118.

[23] Sall B (2007) Beyond the baby boomers: the rise of Generation Y. Australia: KPMG.

[24] Lodes ME (2010) Are Generation Y (Millennial) consumers brand loyal and is their Buying Behaviour affected in an economic recession? A Preliminary Study. 5th Annual Siena

College Student Conference in Business (p. 9). Siena College.
[25] Casidy R (2012) An empirical investigation of the relationship between personality traits, prestige sensitivity, and fashion consciousness of Generation Y in Australia. Australasian Marketing Journal, 20: 42-49.
[26] Maria N (2012) Generation Y and Luxury Brands: A high stake rendez-vous. Luxe Avenue- Sourcing Talent in Lu'1lry, Luxe Avenue.
[27] Saxena P, Jain R (2012) Managing Career Aspirations of Generation Y at Work Place. International Journal of Advanced Research in Computer Science and Software Engineering, 2 (7), 114-118. 2012.
[28] Rahulana M, Troynikov O Watsona C, Jantab M Sennerb V (2013) Consumer purchase behaviour of sports compression garments-A study of Generation Y and Baby Boomer cohorts. Procedia Engineering, 163-169.
[29] Parment A (2013) Generation Y vs. BabyBoomers: Shopping behavior, buyer involvement and implications for retailing. Journal of Retailing and Consumer Services, 20: 189-199.
[30] Valentine D, Powers T (2013) Online product search and Purchase behavior of Generation Y. Atlantic Marketing Journal 2: 76-91.
[31] Kuruvilla SJ, Joshi N (2010) Influence of demographics, psychographics, shopping orientation mall shopping attitude and purchase patterns on mall patronage in India. Journal of Retailing and Consumer Services, 17: 259-269.
[32] Pentecost R, Andrews L (2010) Fashion retailing and the bottom line: The effects of generational cohorts gender fashion fanship, attitudes and impulse buying on fashion expenditure. Journal of Retailing and Consumer Services, 17: 43-52.

INFOGAIN PUBLICATION

International Journal of Advanced Engineering, Management and Science (IJAEMS)
Peer-Reviewed Journal
ISSN: 2454-1311 | Vol-10, Issue-2; Feb, 2024
Journal Home Page: https://ijaems.com/
DOI: https://dx.doi.org/10.22161/ijaems.102.2

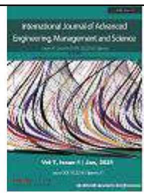

Green synthesis of iron-organic framework Fe-BTC using direct ultrasound to remove methylene blue dye

Nam Ho Phung Khac

[1]Institute of Chemistry and Materials, No. 17 Hoang Sam Street, Cau Giay District, Ha Noi, Vietnam
Email: homyhu@gmail.com

Received: 05 Jan 2024; Received in revised form: 10 Feb 2024; Accepted: 20 Feb 2024; Available online: 28 Feb 2024

***Abstract*— *Metal-organic framework materials (MOFs) comprise organic bridges and metal centers (as connection points). MOFs have unique properties such as crystal structure, large specific surface area, flexible structural framework, and can change the size and shape of pores and diverse chemical functional groups inside the pores. In this study, metal-organic framework materials based on iron (Fe) and the organic ligand H_3BTC were successfully synthesized by ultrasonic method and evaluated for their ability to remove MB dye through Investigate the effects of MB concentration, pH, isotherm model, and adsorption kinetics. With a size of about 100 - 200 nm and an excitation wavelength in the ultraviolet region, the synthesized material shows potential in environmental treatment when the adsorption efficiency reaches over 60% after just 10 minutes and over 80% both processes under sunlight conditions. In addition, the synthesized material is also evaluated to have selective adsorption with Methylene Blue dye.*

***Keywords*—Metal-organic frameworks, removing dye, methylene blue, treatment wastewater.**

I. INTRODUCTION

In recent years, industrial wastewater from textile industries containing many organic pigments has become a severe problem in developing countries [1]. Most organic colors are chemically stable, difficult to decompose, and can destroy the environment if not handled properly [2]. In particular, Methylene Blue (MB) is a popular organic colorant in the textile industry [3]. This type of organic pigment has a long-term impact on the environment due to its ability to block sunlight from entering the aquatic environment, thereby affecting living organisms. On the other hand, for public health, MB can cause eye burns and permanent damage. It produces a burning sensation if swallowed, leading to nausea [4]. Therefore, advanced technology to treat wastewater from dye production is exciting. Up to now, a series of wastewater treatment technologies have been developed, such as biodegradation [5], physical adsorption [6], chemical reaction [7], etc. In advanced oxidation processes, photocatalytic degradation technology is highly effective in decomposing organic pigments into less toxic or biodegradable molecules or even minerals. Transform them into less harmful substances such as CO_2 and H_2O under sunlight and have more economical treatment costs [8, 9].

The current potential type of material for environmental treatment based on adsorption and photocatalysis mechanisms is organometallic framework materials (MOFs) [10]. Compared with traditional system photocatalysts, MOF materials have many advantages in improving photocatalytic efficiency due to their high topology and surface area, which are favorable for the rapid migration and accumulation of organic dye molecules [11]. In particular, iron-based metal-organic framework materials (Fe-MOFs), an essential branch of MOFs, not only have topological properties and a high specific surface area similar to many other MOF materials but are also more environmentally friendly [12]. The methods for synthesizing Fe-MOF materials are very diverse. Among those methods, the solvothermal method is mainly used, but ultrasound-based synthesis is preferred because it saves synthesis time and energy [13]. During ultrasound, periodic mechanical vibrations with large wavelengths interact with the liquid, creating sudden pressure fluctuations. The bubbles forming, growing, and collapsing inside these points lead to localized hot zones with extremely high temperatures and pressures, creating favorable conditions for chemical reactions in a solution containing precursors and forming material structures [14].

In this study, metal-organic framework materials based on iron (Fe) were synthesized by direct ultrasonic method with green water solvent. It was evaluated for structural characteristics and decomposition ability with MB organic pigment. Among them, the organic ligand 1,3,5-benzene dicarboxylate (BTC), one of the most versatile ligands for synthesizing MOFs thanks to its different binding sites [15], was used to construct MOFs. Build the structural framework of the material.

II. EXPERIMENTS

Chemicals

Iron (III) chloride hexahydrate ($FeCl_3.6H_2O$, 99%, Xilong, China); 1,3,5-benzenetricarboxylic acid (H_3BTC, 98%, Macklin, China); Ethanol (C_2H_6O, 95%, Macklin, China); Sodium hydroxide (NaOH, 99%, Macklin, China); Hydrochloric acid (HCl, 37%, Xilong, China); distilled water.

Synthesis of Fe-BTC material

First, 5.4 grams of $FeCl_3.6H_2O$ material were wholly dissolved in 200 ml of distilled water, and 2.8 grams of H_3BTC material were added and then stirred well on a magnetic stirrer at a speed of 400 rpm. After stirring for 30 minutes, the solution system was sonicated with an operating capacity of 1440W run/rest pulse of 10 seconds/5 seconds for 10 minutes. The product was then centrifuged, the solution removed, washed several times with ethanol, and then dried at 120 ^oC for 6 hours.

Characterizations

Scanning electron microscopy Hitachi S-4600 was employed to observe particle size and morphology. An X'Pert PRO PANalytical instrument with a radiation source of 0.154 nm CuK_α has obtained XRD patterns for all samples. Fourier transform infrared spectroscopy (FTIR, TENSOR II, Bruker) was used to investigate the surface functional groups of the MOF material. The N_2 adsorption isotherm at 77 K using a BET TriStar II Plus 377 was employed to calculate the surface area of the material.

Removal of methylene blue

The experiments were conducted with the ratio of Fe-BTC material to the amount of MB solution of 0.5 g per litter. The Fe-BTC material and the MB solution were put into a transparent glass tube, sealed with a tight cap, and put into a closed dark box to study the MB adsorption capacity of the material. For the experiment to evaluate the simultaneous adsorption-catalysis ability, the tube is put under simulated sunlight by Xenon lamp. After the time needed to survey, filter out the material from the solution to analyze the MB concentration by UV-Vis photometric method on a UV-Vis DV-8200 device (Drawell).

The equation for the determination of MB concentration was built as follows:

$$C = 6.2933Abs + 0.12955 \quad (1)$$

with (λ = 664 nm, R^2 = 0.9983).

Where, C is the concentration of MB in the solution, mg/L. Abs is the intensity of light absorption. R^2 is the correlation coefficient of the empirically constructed standard curve equation.

The formula calculated the MB removal efficiency of the material:

$$H(\%) = \frac{(C_0 - C_t)}{C_0} \times 100 \quad (2)$$

The adsorption capacity was calculated according to the procedure:

$$q_t\,(mg/g) = \frac{V \times (C_0 - C_t)}{m} \quad (3)$$

Where, C_0, C_t are MB (mg/L) concentrations initially and at time t; V is the volume of MB solution (L); m is the mass of material Fe-BTC (g).

III. RESULTS AND DISCUSTION

Characterization of Fe-BTC

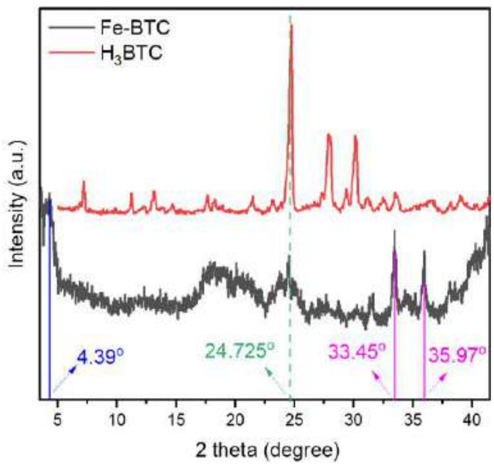

Fig. 1: X-ray diffraction pattern of the Fe-BTC by ultrasound.

The structural phase characteristics of the synthesized material are shown in Fig. 1. The signal intensity of the XRD spectrum shows that the material has poor crystallization. However, the presence of H_3BTC material at position 24.725° can be assessed initially. Besides, a unique diffraction peak appears at position 4.39°, corresponding to the (001) lattice of the monoclinic crystal system in the material $Fe_4O_{12}C_{116}H_{128}$ [16]. Although no characteristic peak exists at the angular position 5° to 15°, the synthesized material exhibits a broadened peak from 16° to 22.5°. The impact on this structure may be due to the nano size of the material [17] or the existence of some α-Fe_2O_3 particles [18]. The 33.45° and 35.97° peaks correspond to the standard spectrum 96-901-4881.

The morphology of the synthesized material is shown in Fig.2. The particle material was evaluated with sizes ranging from 100 to 200 nm. At the same time, the material system agglomerates together due to the influence of the magnetic material α-Fe_2O_3 [19], but this accumulation is not significant.

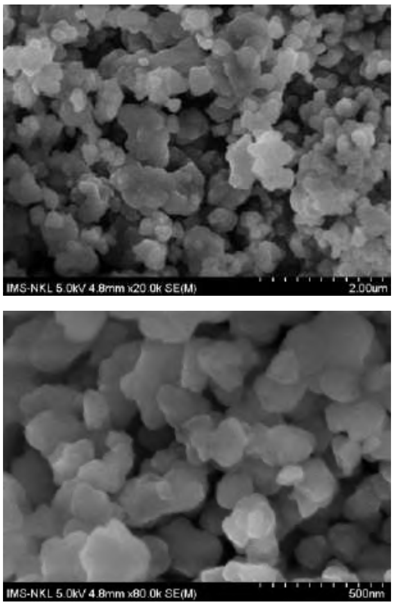

Fig. 2: Scanning electron microscopy (SEM) images of Fe-BTC by ultrasound.

The FTIR spectrum of the synthesized material and H_3BTC is shown in Fig. 3. In the spectrum of the Fe-BTC material, a broadened peak appears at the wavenumber position of about 3400 cm^{-1}, representing the OH group vibration of the molecules. Water molecules are adsorbed on the surface [20]. The peaks at positions 1627 cm^{-1} and 1574 cm^{-1} represent asymmetric stretching vibrations of the carboxylate group in the organic ligand BTC. In addition, the symmetric vibrations of this group are also shown at two peaks at 1376 cm^{-1} and 1450 cm^{-1}. The peaks at wave number 710 - 757 cm^{-1} represent the CH bond of the aromatic ring. In particular, the peaks at positions 459 - 479 cm^{-1} represent the Fe-O vibrations of the material [17, 20, 21].

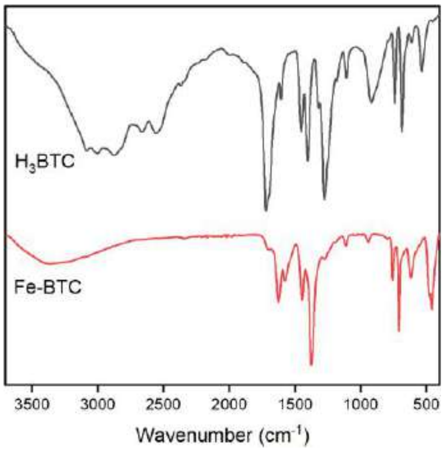

Fig. 3: FTIR spectra of Fe-BTC by ultrasound.

N_2 adsorption isotherm research is used to predict the adsorption capacity of Fe-BTC material. The N_2 adsorption-desorption diagram of Fe-BTC is recorded in Fig. 4. The BET surface area of the Fe-BTC sample was 259.846 m^2/g.

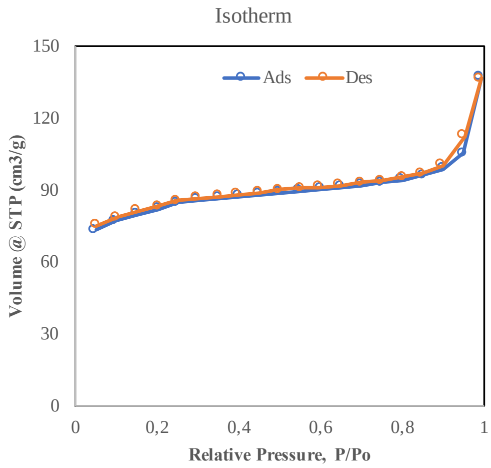

Fig. 4: FTIR spectra of Fe-BTC by ultrasound.

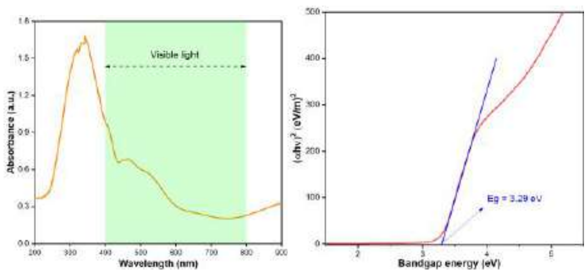

Fig. 5: The UV-Vis spectrum of Fe-BTC by ultrasound.

From the characteristic properties analyzed above, the research team confirmed that they have successfully synthesized the metal-organic framework material Fe using the organic ligand BTC. On the other hand, for applications in the field of adsorption and photocatalysis, parameters related to the optical band gap of the material are critical to determine the optical activity of the material [22]. Using the Tauc method [23], the calculated width energy is about 3.29 eV (Fig. 5), equivalent to the excitation wavelength in the ultraviolet region.

Removal of methylene blue

The material's ability to process MB over time in dark conditions (adsorption) and sunlight conditions (adsorption - photocatalysis) with a Fe-BTC mass of 10 mg per 20 mL of MB solution with a concentration of 10 mg/L is shown in Fig. 6. In general, the efficiency of photocatalytic adsorption treatment is much higher than that of adsorption treatment, about 16 - 31% for each measurement time. For adsorption-photocatalytic treatment, the efficiency reaches 61.48% after 10 minutes and reaches adsorption equilibrium after 60 minutes with an efficiency of about 86%. Meanwhile, adsorption treatment got 30% after 10 minutes and nearly 70% after 60 minutes.

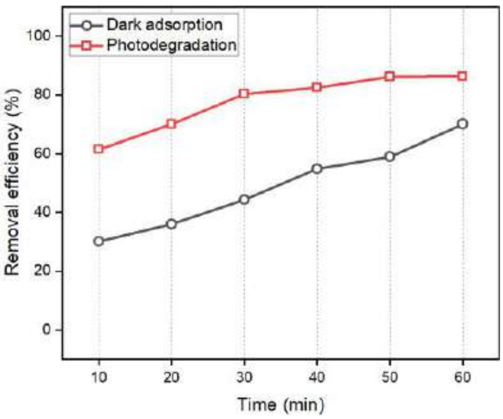

Fig. 6: Adsorption performance of Fe-BTC by ultrasound.

The influence of pH on MB removal efficiency was evaluated in the range from 3 to 11 (adjusting the pH of the stock MB solution with 1 M HCl and 1 M NaOH solutions). The chart evaluating the influence of pH (Fig. 7a) shows that MB treatment efficiency under light conditions is significantly higher than under dark conditions. At the same time, through analysis of Fig. 7b, it is found that the material achieves the highest MB treatment efficiency at pH = 7 in dark conditions. The equilibrium MB removal efficiency increases when pH increases from 3 to 7 because, in acidic environments, many H^+ ions exist that can compete with harmful cations separated from MB, reducing adsorption performance [24]. On the other hand, when the pH value increases from 7 to 11, the adsorption efficiency and capacity decrease due to the reaction between MB-S^+Cl and NaOH in the solution to form a solution containing MB-S^+OH and NaCl. NaCl salt has been shown to reduce the adsorption process of MB-S^+OH on the surface of adsorbent materials [25]. The treatment efficiency is similar for lighting conditions when increasing pH from 3 to 7. However, when increasing the pH value from 7 to 9, the treatment efficiency drops sharply from 85.1% to about 59.0 % and then increases significantly to 87.67% at pH 11. It can be explained by the fact that in a solution of pH 9 and under solid illumination, the reaction between MB and NaOH occurs strongly, causing the adsorption efficiency to decrease. However, when increasing the pH to 11 and under the influence of solid light, MB's dimerization process occurs, shifting the maximum peak from 662 nm to about 610 nm (Fig. 7c).

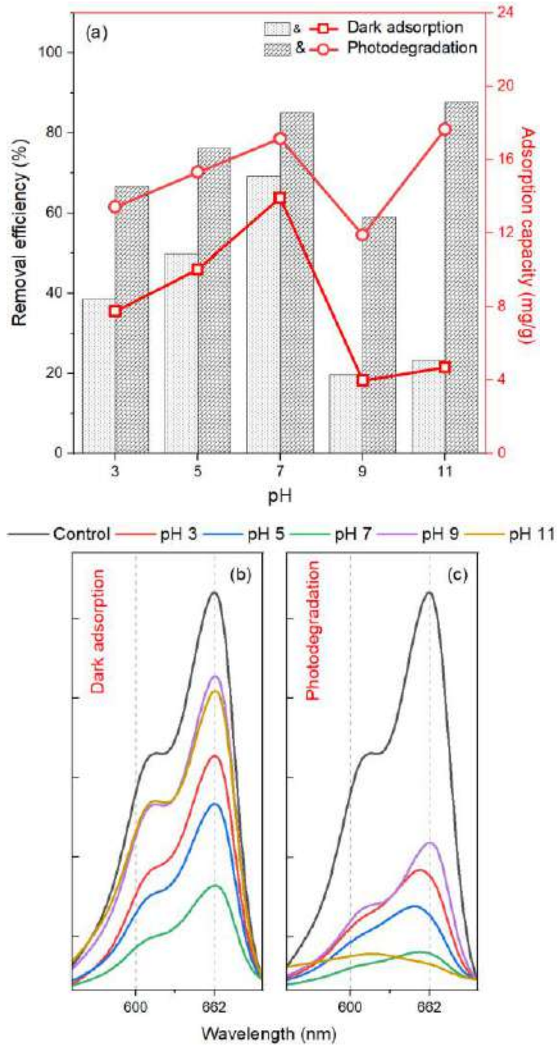

Fig. 7: Effect of pH on the ability to treat MB (a), UV-Vis spectrum of MB solution after adsorption treatment (b), and adsorption - photocatalysis (c).

Three isotherm equations are applied to study the interaction between the adsorbent and adsorbate: Langmuir, Freunlich, and Temkin. The correlation coefficient R^2 values in Fig. 8 show that the adsorption data of FeBTC material is in good agreement with the Freunlich model. Proving that the adsorption process is multilayer on heterogeneous surfaces [26]. In addition, the parameters of the models are summarized in Table 1.

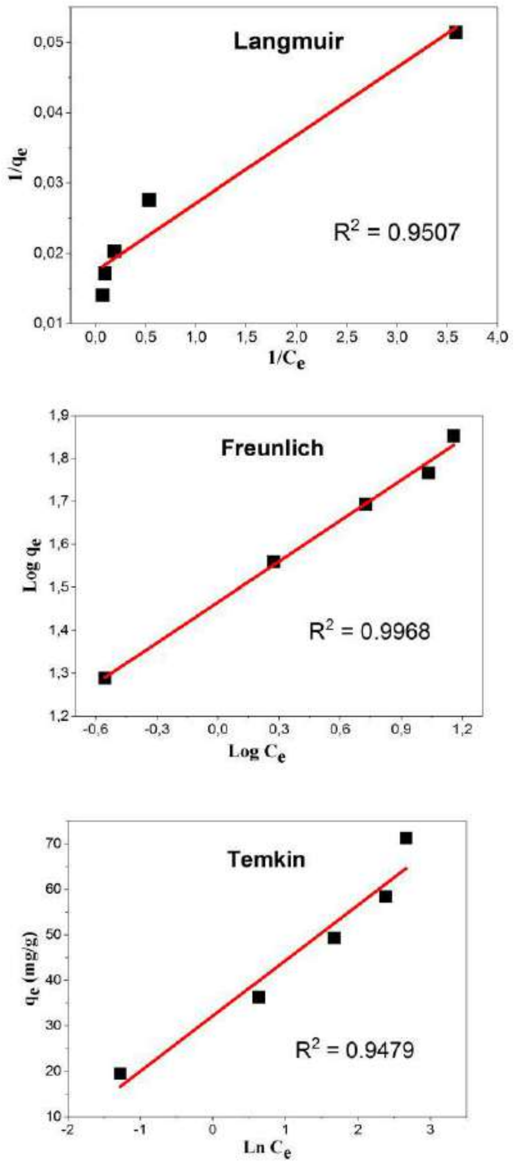

Fig. 8: Adsorption isotherm of the Fe-BTC toward MB.

Table 1: Adsorption isotherm parameters of Fe-BTC by ultrasound.

Model	Equation	Parameters
Langmuir	$\frac{C_e}{q_e} = \frac{1}{K_L \cdot q_m} + \frac{C_e}{q_m}$	q_{max} = 57.30659 (mg/g) K_L = 1.804 (L/mg) R_L = 0.052506 R^2 = 0.9507
Freunlich	$\ln q_e = \ln K_F + \frac{1}{n} \ln C_e$	n = 3,1656 K_F = 29.20452 (mg/g) R^2 = 0.9968
Temkin	$q_e = B_t \ln K_t + B_t \ln C_e$	B_t = 12 , 1745 (J/mol) K_t = 14 .02186 (L/mg) R^2 = 0.9479

The adsorption kinetics of the material were studied through first- and second-order kinetic models at an initial MB concentration of 10 mg/L. Based on the correlation coefficient of the two linear lines, it is found that the material's kinetic model is more compatible with the first-order kinetic model than the second-order kinetic model (Fig. 9).

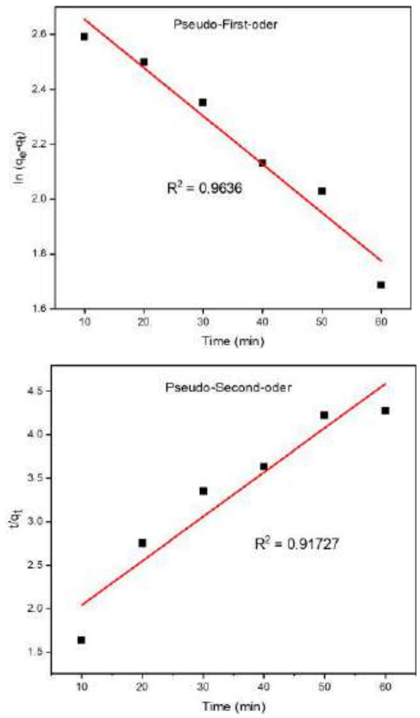

Fig. 9: The kinetic models of Fe-BTC adsorption toward MB.

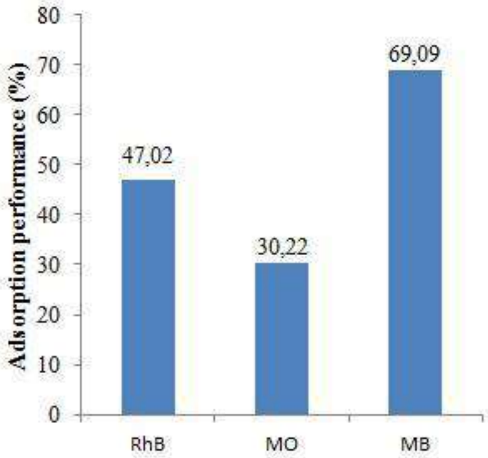

Fig. 10: Adsorption performance of Fe-BTC materials for different dyes after 60 minutes.

Finally, to evaluate the adsorption selectivity, two solutions containing the dyes Methyl Orange (MO) and Rhodamine B (RhB) with the same volume of 20 mL and concentration of 10 mg/L were tested during the adsorption 60-minute period. Based on Fig. 10, it is seen that Fe-BTC material can adsorb dye MB more optimally than the others because the adsorption efficiency after 60 minutes with RhB and MO is 47.02% and 30.22%, respectively. Meanwhile, under the same survey conditions, the MB adsorption efficiency of this material is 69.09%. Survey results show that Fe-BTC material can adsorb all three families of dyes with decreasing levels in the order MB > RhB > MO.

IV. CONCLUSION

This research has successfully synthesized the iron-organic framework material with water as a green solvent by direct ultrasound. Fe-BCT in granular form with a size of about 100 - 200 nm determined the excitation light wavelength of the material in the ultraviolet region. Experimental evaluation of the ability to decompose MB pigment shows that the material has an adsorption efficiency of up to 60% in 60 minutes in dark conditions and over 80% in 60 minutes in sunlight conditions. The adsorption process of the determined material is better compatible with the Freunlich isotherm model and first-order adsorption kinetics. In addition, the material also shows better adsorption selectivity with MB than MO and RhB.

ACKNOWLEDGEMENTS

This research is conducted and funded by Department of Inorganic Materials, Institute of Chemistry and Materials.

REFERENCES

[1] Tianqi Liu, Chukwunonso O. Aniagor, Marcel I. Ejimofor, Matthew C. Menkiti, Yakubu M. Wakawa, Jie Li, Rachid Ait Akbour, Pow-Seng Yap, Sie Yon Lau, Jaison Jeevanandam (2023). Recent developments in the utilization of modified graphene oxide to adsorb dyes from water: A review. Journal of Industrial and Engineering Chemistry, 117, 21-37.

[2] F S. Banerjee, P. Benjwal, M. Singh, KKJAss Kar (2018). Graphene oxide (rGO)-metal oxide (TiO_2/Fe_3O_4) based nanocomposites for the removal of methylene blue. Applied Surface Science, 439, 560-568.

[3] Z. Mengting, TA Kurniawan, S. Fei, T. Ouyang, MHD Othman, M. Rezakazemi, SJEP Shirazian (2019). Applicability of $BaTiO_3$/graphene oxide (GO) composite for enhanced photodegradation of methylene blue (MB) in synthetic wastewater under UV–vis irradiation. Environmental Pollution, 255(Part1), 113182.

[4] R. Al-Tohamy, SS Ali, F. Li, KM Okasha, YAG Mahmoud, T. Elsamahy, H. Jiao, Y. Fu, J. Sun (2022). A critical review on the treatment of dye-containing wastewater: Ecotoxicological and health concerns of textile dyes and possible remediation approaches for environmental safety. Ecotoxicology and Environmental Safety, 231, 113160.

[5] K. Qi, Z. Li, C. Zhang, X. Tan, C. Wan, X. Liu, L. Wang, D.J. Lee (2020). Biodegradation of real industrial wastewater containing ethylene glycol by using aerobic granular sludge in a continuous-flow reactor: Performance and resistance mechanism. Biochemical Engineering Journal, 161, 107711.

[6] C. Yin, C. Xu, Y. Jia, W. Sun, C. Wang, G. Zhou, M. Xian (2019). Insight into highly efficient removal of sulfonic acid pollutants by a series of newly-synthesized resins from aqueous media: Physical & chemical adsorption. Journal of the Taiwan Institute of Chemical Engineers, 95, 383-392.

[7] J. Chakraborty, I. Nath, S. Song, S. Mohamed, A. Khan, PM Heynderickx, F. Verpoort (2019). Porous organic polymer composites as surging catalysts for visible-light-driven chemical transformations and pollutant degradation. Journal of Photochemistry and Photobiology C: Photochemistry Reviews, 41, 100319

[8] I. Khan, K. Saeed, N. Ali, I. Khan, B. Zhang, M. Sadiq (2020). Heterogeneous photodegradation of industrial dyes: An insight to different mechanisms and rate affecting parameters. Journal of Environmental Chemical Engineering 8(5), 104364.

[9] C. Feng, Z. Chen, J. Jing, J. Hou (2020). The photocatalytic phenol degradation mechanism of Ag-modified ZnO nanorods. Journal of Materials Chemistry C, 8(9), 3000-3009.

[10] V. García-Salcido, P. Mercado-Oliva, JL Guzmán-Mar, BI Kharisov, L. Hinojosa-Reyes (2022). MOF-based composites for visible-light-driven heterogeneous photocatalysis: Synthesis, characterization and environmental application studies. Journal of Solid State Chemistry, 307, 122801.

[11] Y. Bai, S. Zhang, S. Feng, M. Zhu, S. Ma (2020). The first ternary Nd-MOF/GO/Fe_3O_4 nanocomposite exhibiting an

excellent photocatalytic performance for dye degradation. Dalton Transactions, 49(31), 10745-10754.

[12] G. Zhu, S. Wang, Z. Yu, L. Zhang, D. Wang, B. Pang, W. Sun (2019). Application of Fe-MOFs in advanced oxidation processes. Research on Chemical Intermediates 45(7) 3777-3793.

[13] J. Joseph, S. Iftekhar, V. Srivastava, Z. Fallah, EN Zare, M. Sillanpää (2021). Iron-based metal-organic framework: Synthesis, structure and current technologies for water reclamation with deep insight into framework integrity. Chemosphere, 284, 131171.

[14] C. Vaitsis, G. Sourkouni, C. Argirusis (2019). Metal Organic Frameworks (MOFs) and ultrasound: A review. Ultrasonics Sonochemistry, 52, 106-119.

[15] [15] A. Sarkar, A. Adhikary, A. Mandal, T. Chakraborty, D. Das (2020). Zn-BTC MOF as an Adsorbent for Iodine Uptake and Organic Dye Degradation. Crystal Growth & Design, 20(12) ,7833-7839.

[16] JA Carmona-Negrón, A. Santana, AL Rheingold, E. Meléndez (2019). Synthesis, structure, docking and cytotoxic studies of ferrocene–hormone conjugates for hormone-dependent breast cancer application. Dalton Transactions, 48(18), 5952-5964.

[17] P. Horcajada, S. Surblé, C. Serre, D.-Y. Hong, Y.-K. Seo, J.-S. Chang, J.-M. Grenèche, I. Margiolaki, G. Férey (2007). Synthesis and catalytic properties of MIL-100(Fe), an iron(iii) carboxylate with large pores. Chemical Communications, (27), 2820-2822.

[18] N. Armon, E. Greenberg, E. Edri, A. Kenigsberg, S. Piperno, O. Kapon, O. Fleker, I. Perelshtein, G. Cohen-Taguri, I. Hod, H. Shpaisman (2019). Simultaneous laser-induced synthesis and micro-patterning of a metal organic framework. Chemical Communications, 55(85), 12773-12776

[19] V. Ramalingam, M. Harshavardhan, S. Dinesh Kumar, S. Malathi Devi (2020). Wet chemical mediated hematite α-Fe2O3 nanoparticles synthesis: Preparation, characterization and anticancer activity against human metastatic ovarian cancer. Journal of Alloys and Compounds, 834(5), 155118-155128.

[20] NK Gupta, J. Bae, KS Kim (2021). Iron-organic frameworks-derived iron oxide adsorbents for hydrogen sulfide removal at room temperature. Journal of Environmental Chemical Engineering, 9(5), 106195.

[21] AA Castañeda Ramírez, E. Rojas García, R. López Medina, JL Contreras Larios, R. Suárez Parra, AM Maubert Franco (2021). Selective Adsorption of Aqueous Diclofenac Sodium, Naproxen Sodium, and Ibuprofen Using a Stable Fe3O4–FeBTC Metal–Organic Framework. Materials, 14(9), 2293.

[22] P. Makuła, M. Pacia, WJTjopcl Macyk (2018). How To Correctly Determine the Band Gap Energy of Modified Semiconductor Photocatalysts Based on UV–Vis Spectra. The Journal of Physical Chemistry Letters, 9(23), 6814-6817.

[23] K. Fabrizio, KN Le, AB Andreeva, CH Hendon, CKJAML Brozek (2022). Determining Optical Band Gaps of MOFs. ACS Materials Letters, 4(3), 457-463.

[24] Y. Xu, J. Jin, X. Li, C. Song, H. Meng, X. Zhang (2016). Adsorption behavior of methylene blue on Fe3O4-embedded hybrid magnetic metal–organic framework. Desalination and Water Treatment, 57(52), 25216-25225.

[25] JO Amode, JH Santos, Z. Md. Alam, AH Mirza, CC Mei (2016). Adsorption of methylene blue from aqueous solution using untreated and treated (Metroxylon spp.) waste adsorbent: equilibrium and kinetics studies. International Journal of Industrial Chemistry, 7(3), 333-345.

[26] VO Shikuku, T. Mishra (2021). Adsorption isotherm modeling for methylene blue removal onto magnetic kaolinite clay: a comparison of two-parameter isotherms. Applied Water Science, 11(6), 103.

International Journal of Advanced Engineering, Management and Science (IJAEMS)
Peer-Reviewed Journal
ISSN: 2454-1311 | Vol-10, Issue-2; Feb, 2024
Journal Home Page: https://ijaems.com/
DOI: https://dx.doi.org/10.22161/ijaems.102.3

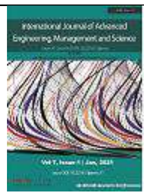

Effect of Replacement Layers on Bearing Capacity of Silty Clay Layer

Mohamed A. Jpr, Alnos A. Easa, Elsayed A. El-Kasaby

Dep. Of Civil Eng., Faculty of Engineering, Banha University, Egypt
•Corresponding author, E-mail: Eng.mohamed.japr@gmail.com

Received: 02 Jan 2024; Received in revised form: 07 Feb 2024; Accepted: 18 Feb 2024; Available online: 28 Feb 2024

***Abstract*— *Soil conditions often pose significant challenges for soil and foundation engineers engaged in construction projects. In response to these challenges, researchers and engineers have dedicated considerable efforts to developing solutions to construct on weak soil layers. The replacement layer is one of the most efficient and effective methods to increase the ultimate bearing capacity under foundation. There are many advantages for replacement layer using such as its low cost, material availability, easy construction, quick construction time, simple testing procedures. There is a few of studies that determine the actual values of the ultimate bearing capacity of replacement layers. Most research and studies focus on theoretical and mathematical values of the ultimate bearing capacity for foundations replacement layers. The site selected for this study was located in Al-Qalyubia Governorate. The use of replacement layers in this study indicated that there is an increase in the ultimate bearing capacity for the studied site. In addition to that, engineering properties of replacement layer and natural soil condition plays a role in the ultimate bearing capacity values.*

Keywords*— Soil Conditions, Replacement Layer, Ultimate Bearing Capacity, Construction Solutions, Engineering Properties

I. INTRODUCTION

The foundation is recognized for transmitting the structure's weight and other loads to the soil beneath it. These loads must be transmitted in such a way that the soil's capacity to hold the loads is not exceeded. To put it another way, a scientific foundation design must be based on the soil's carrying capacity [4],[12],[14] [19], and [20].

Ashraf [1], Coduto [3], Tomlinson [16], and Winterkorn [18] stated that, Layers of replacements are usually carried out with soil stronger than the original soil or at least equal to it. It is carried out in layers whose thickness does not exceed 30 cm. The main purpose to use replacement layers in the construction works as the following:

1. Rise the foundation level.
2. Increasing the bearing capacity of the soil under foundation.
3. Keeping away the structures from the area of groundwater influence or protecting foundations from ground water effects.
4. Reduce the effects of elastic soil layers such as swelling soil layers.
5. Reduce the effect of rigidity between foundation and hard soil layers such as rock soil.
6. Reduce the vertical stresses on the original soil.

As for the type of soil used in the replacement, it must be free from all the previous defects and have no relationship to the replacement soil with the original soil - meaning the replacement layer must be tested on that it is suitable for establishment [2], [4], [12], and [14].

Various types of foundations are used depending on the structure and soil encountered. Spread footing, mat foundation, pile foundation, and drilled shaft foundation are the most popular types of foundations. A spread footing is essentially an extension of a load-bearing wall or column that allows the structure's load to be distributed over a wider area of the soil. The size of the spread footings needed in low-load-bearing soil is impractically high. in that case, constructing the whole structure on a concrete pad is more cost-effective [7], [15], and [17].

Bearing capacity is the ultimate load a soil layer can support before shear failure. Settlement, on the other hand, refers to the downward movement of a structure due to soil compression under applied loads [10], and [8].

The bearing capacity calculation methods are based on theoretical considerations developed to reflect experimental observations. In case of different value of bearing capacity, using plate load test is the ideal solution to identify the more realistic value of it. In case of low bearing capacity of the soil layer, the replacement layers may be suggested to improve the bearing capacity [8], and [9].

II. THE STUDIED SITE

The site was chosen for this study where the natural soil layers is cohesive soil layers for present study purpose. the site was investigated to determine the soil classification and soil physical properties by Egyptian Military Technical Collage. **Error! Reference source not found.** shows the location of the studied site which was chosen for the experimental works. the two is located in Qalyubia Governorate, where it contains (Silty clay soil) in the land of El-Awkaf - Shubra Al-Khaima - Qalyubia Governorate - Greater Cairo. It is 200 meters from the Road Ring, and in the middle is the axis of 15 May. Soil properties of the site determined by the soil props done by the Egyptian Military Technical College, was planned for the construction of 883 social housing units. The site was planned with three building models (i) Model A: 6 floors (ground floor + 5 floors); (ii) Model B: 8 floors (ground floor + 7 floors); (iii) Model C: 10 floors (ground floor + 9 floors).

The physical and mechanical properties of the soil layers were determined to classify the soil types and soil stratifications. The engineering tests were carried out in the Soil Mechanics and Foundations Laboratory of the Faculty of Engineering, Military Technical Collage. Therefore, at the site, the Egyptian Military Technical College recommended that the excavation to a depth of 3 meters and use of replacement layers with a thickness of 1.5 meters of gravel and sand at a ratio of 1:1. So that, the replacement layers they are placed on layers of no more than 25 cm in thickness, taking into account, their immersion and compaction, using a masher of not less than 15 tons. The engineering properties of the fine soil layer at different depths are listed in Table 1 such as natural density, natural water content, specific gravity, etc. It is clear that, the index properties of natural fine soil are excessively the same values. According to unified classification system (most common used) and by using plasticity chart, it is noted that, the soil up to depth 9.0m from ground surface can be classified as CH. Where, CH represents clay of high plasticity.

Table 1: Index properties of silty clay soil

Depth (m)	3.0	6.0
Natural unit Weight of soil γ (t/m3)	1.66	1.68
Natural Water Content wc (%)	28	31
Liquid limit L.L (%)	51	53
Plastic Limit PL (%)	28	27
Plasticity index PI (%)	23	26
Shrinkage limit SL (%)	16.5	17
Specific gravity Gs	2.71	2.70
Free swell F.S. (%)	75	100
Degree of Saturation S (%)	95	100
Soil Classification	CH	CH

Fig. 1: Location of the site

2.1 Properties of Replacement layers

Due to the recommendation of Egyptian Military Technical Collage report to use replacement layer materials as the mixed of crushed stone and sand with 1:1 ratio. With the knowledge of the commander of the supervision staff from the

Engineering Authority of the Egyptian Armed Forces, samples of siliceous sand and crushed stone were provided from private quarries of the Egyptian Armed Forces.

In addition to that, the sieve analysis curves of crushed stone and sand material are shown in **Error! Reference source not found.**, and **Error! Reference source not found.**. Also, the engineering properties of crushed stone as the general visual characterization of crushed stone samples of various sizes is white to light brown. The natural water content, volumetric weight, specific gravity of grains, gradient coefficient, uniformity coefficient is recorded in

Gravel			Sand			Silt			Clay	Gravel	Sand	Silt	Clay
Coarse	**Medium**	**Fine**	**Coarse**	**Coarse**	**Medium**	**Fine**	**Coarse**	**Medium**			**Coarse**	**Medium**	**Fine**

Table 2, and

Table *3*.

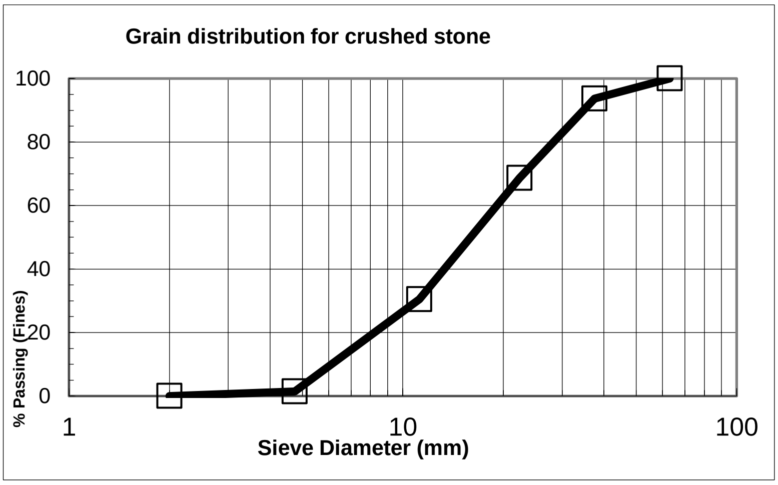

Fig. 2: Granular gradient curve for the crushed stone used in the replacement layers

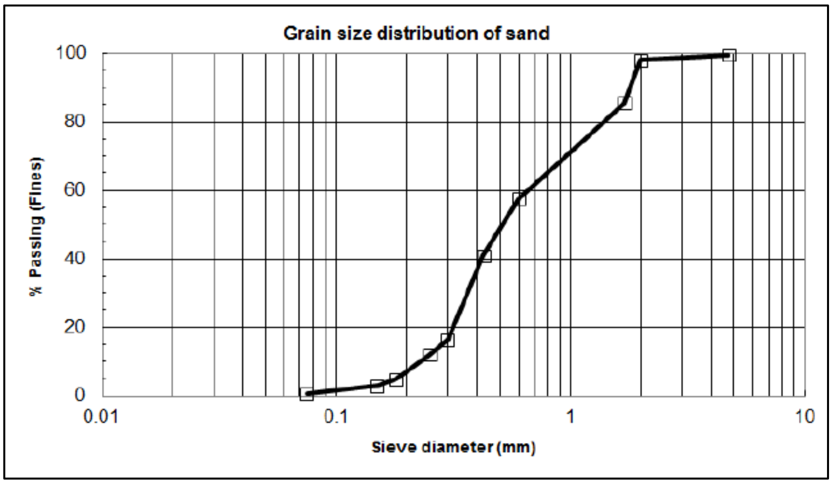

Fig. 3: Granular gradient curve for the sand used in the replacement layers

Gravel	Sand	Silt	Clay		Gravel	Sand	Silt	Clay

Coarse	Medium	Fine	Coarse	Coarse	Medium	Fine	Coarse	Medium			Coarse	Medium	Fine	

Table 2: Geometrical properties of crushed stone samples

$w_{nat.}$	G_s	Gravel	Sand	Fines	C_u	C_c
1.10 %	2.67	98.0 %	2.0 %	0.0 %	3.03	1.61

Table 3: Geometrical properties of sand samples

$w_{nat.}$	G_s	Gravel	Sand	Fines	C_u	C_c
1.72 %	2.68	1.5 %	98.2 %	0.3 %	2.82	0.75

2.2 Compaction Test

In the laboratory, the modified compaction test of the mixture of crushed stone and sand (1:1) was carried out using a modified Proctor device to determine the maximum dry density ($\gamma_{dmax.}$) and the optimum moisture content (OMC). Fig. 4 completes the results of the tests. Accordingly, the compaction parameters are record as, $\gamma_{dmax} = 2.10\ gm/cm^3$, and $OMC = 6.15\%$

In field, Table 4 show the values of moisture content (%), dry density (g/cm^3) and degree of compaction (%) for each replacement layer separately and for both sites, in order.

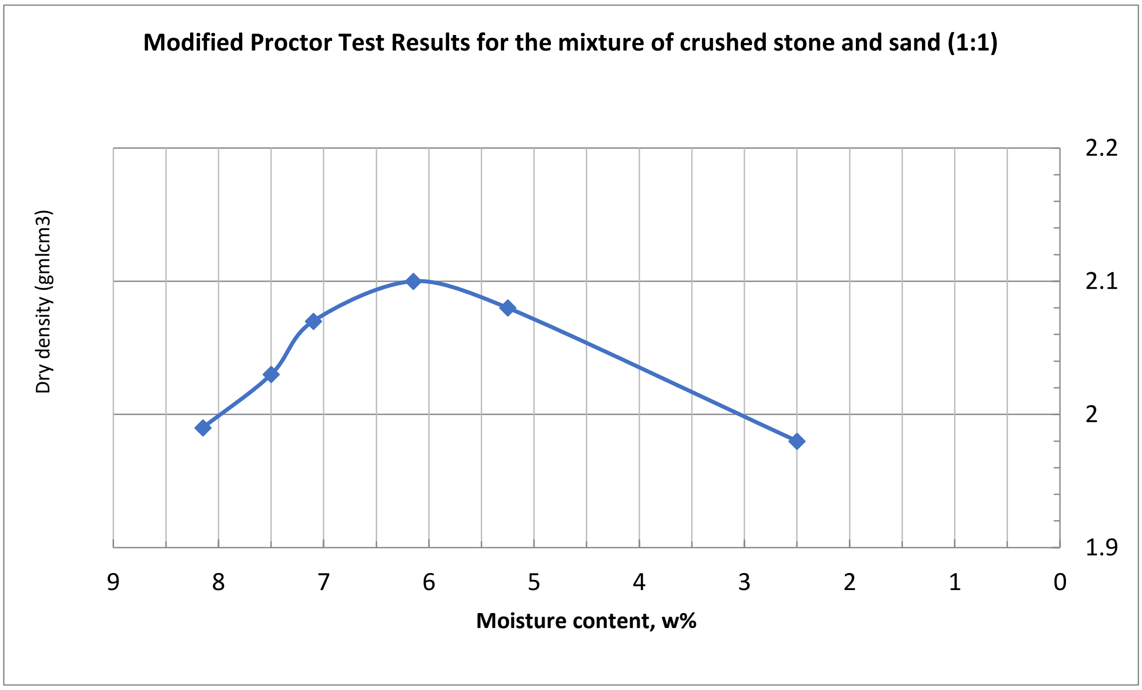

Fig. 4: Lab-Modified Compaction Test Results

Table 4: The average values of field compaction test, crushed stone and sand mixture (1:1) replacement layers

Layer No.	Layer 1	Layer 2	Layer 3	Layer 4	Layer 5	Layer 6	Average
Moisture content (%)	7.10	7.24	5.66	6.75	7.04	5.80	6.60
Dry density (gm/cm^3)	2.08	2.14	2.02	2.14	2.06	2.08	2.09
Compaction degree (%)	99	102	96	102	98	99	99.33

2.3 Plate Loading Test

The engineering tests and their measurements were earned out and evaluated according to Egyptian Code [5] or by the manner of testing as mentioned in soil mechanics handbooks as Bowles [2], El-Kasaby [6], Perkins [11], and Reznik [13]. The site contains many buildings. The excavation level from ground surface is 3m (D = -3m). It was suggested that using replacement layer of 1.5m thickness. Replacement layer constructed as 6 layers (each one 25cm) and compacted, as listed in

Table 5.

Plate bearing tests results contain the applied loads Q ton. The applied loads are measured by the gauge of hydraulic jack. For each plate loading tests the obtained results are indicated by curve as the relation between applied load Q and settlement. According to the results of plate loading tests. The ultimate bearing capacity can be estimated.

Table 5: The Conducted Plate loading tests in the Site, for each building area

Test Number	Replacement Layer Number	Level from ground surface (m)	Notes
1	0	-3.00	At excavation layer
2	1	-2.75	R.L. Thickness = 0.25m
3	2	-2.50	R.L. Thickness = 0.50m
4	3	-2.25	R.L. Thickness = 0.75m
5	4	-2.00	R.L. Thickness = 1.00m
6	5	-1.75	R.L. Thickness = 1.25m
7	6	-1.50	R.L. Thickness = 1.50m

III. RESULTS AND DISCUSSION

3.1 Excavation Level

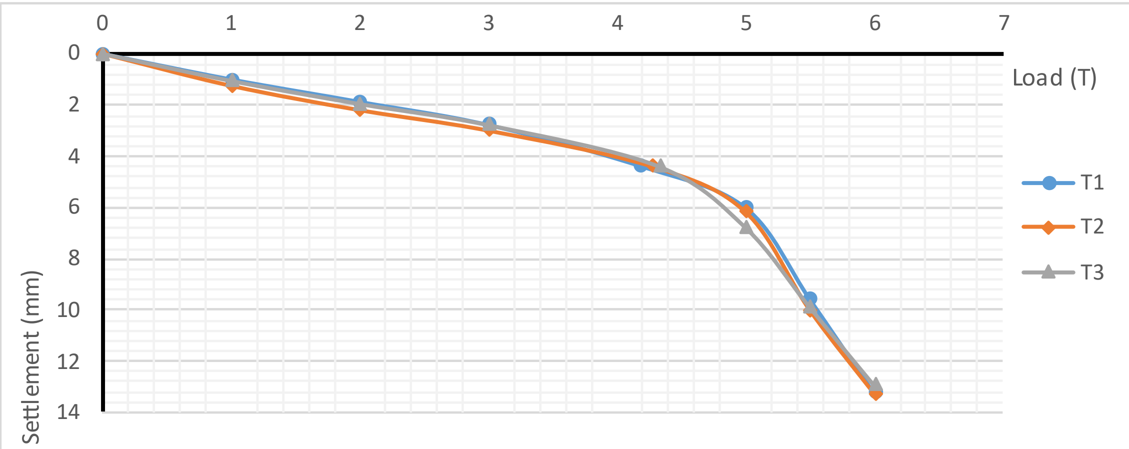

Fig. 5: Plate loading test result at excavation level

The results of plate loading tests on natural soil layer (at level -3m from ground surface) are shown in **Error! Reference source not found.**. It's clear that a gradual decline that occurs to the natural soil. So that the average ultimate bearing capacity for these results is 26.813t/m^2. At test 1 the $q_{ult.}$ = 26.313 t/m^2 at Q_{max} = 4.184 ton, while at test 2 the q_{ult} = 26.907 t/m^2 for Q_{max} = 4.278 ton, and finally the q_{ult} = 27.219 t/m^2 at Q_{max} = 4.328 ton with averages of q_{ult} (average) = 26.813 t/m^2.

3.2 First Replacement Layer Level

In the first replacement layer at level D = -2.75m, the curve in **Error! Reference source not found.** appears almost in the same shape as the curve of the natural soil, the ultimate bearing capacity ($q_{ult.}$) increases by 13.7 % with in perspective to the excavation level. At test 1 the $q_{ult.}$ = 29.108 t/m^2 at Q_{max} = 4.628 ton, while at test 2 the q_{ult} = 28.357 t/m^2 for Q_{max} = 4.509 ton, and finally the q_{ult} = 32.041 t/m^2 at Q_{max} = 5.413 ton with averages of q_{ult} (average) = 29.835 t/m^2.

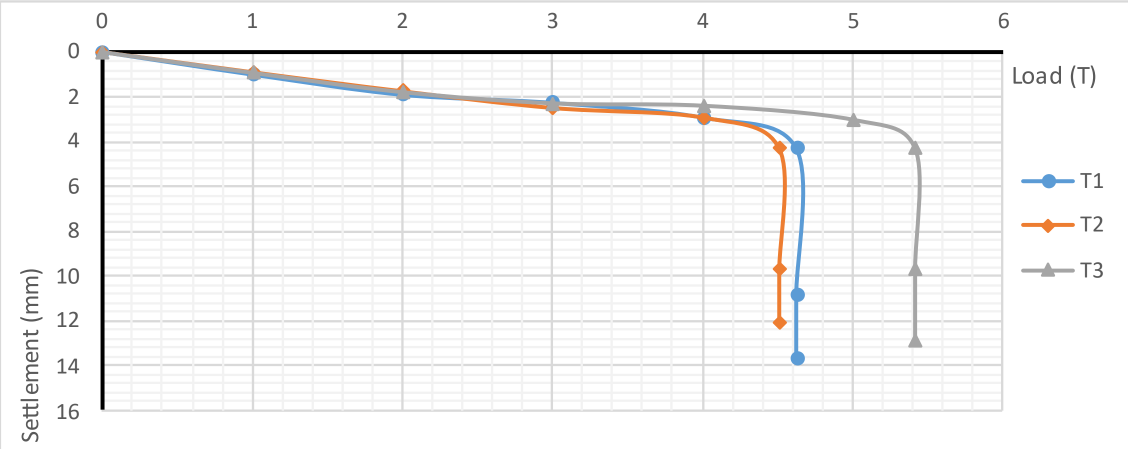

Fig. 6: Plate loading test result at first R.L. level No. (1)

3.3 Second Replacement Layer Level

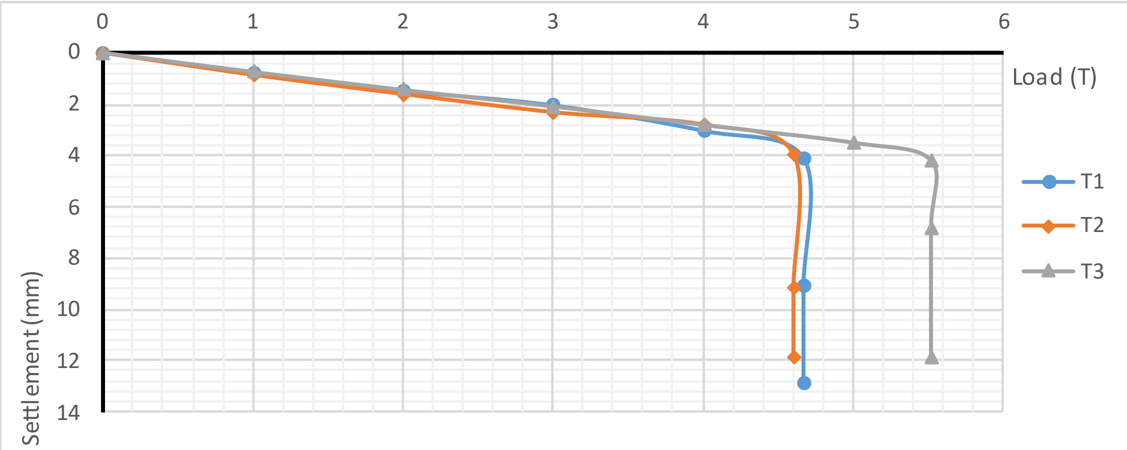

Fig. 7: Plate loading test result at second R.L. level No. (2)

After placing the second replacement layer and reached to (D = -2.5m). It is noted in **Error! Reference source not found.** that the average ultimate bearing capacity for these results increases 15.6% than that obtained from the result of excavation level. At test 1 the $q_{ult.}$ = 29.401 t/m^2 at Q_{max} = 4.675 ton, while at test 2 the q_{ult} = 28.918 t/m^2 for Q_{max} = 4.598 ton, and finally the q_{ult} = 34.687 t/m^2 at Q_{max} = 5.515 ton with averages of q_{ult} (average) = 31.002 t/m^2.

3.4 Third Replacement Layer Level

As illustrated in **Error! Reference source not found.**, The value of the average ultimate bearing capacity after placing the third replacement layer (D = -2.25m) has increased 20%. Knowing that the percentages of increasing and decreasing are proportional to the excavation level. At test 1 the $q_{ult.}$ = 31.664 t/m^2 at Q_{max} = 5.035 ton, while at test 2 the q_{ult} = 32.179 t/m^2 for Q_{max} = 5.116 ton, and finally the q_{ult} = 32.649 t/m^2 at Q_{max} = 5.114 ton with averages of q_{ult} (average) = 32.164 t/m^2.

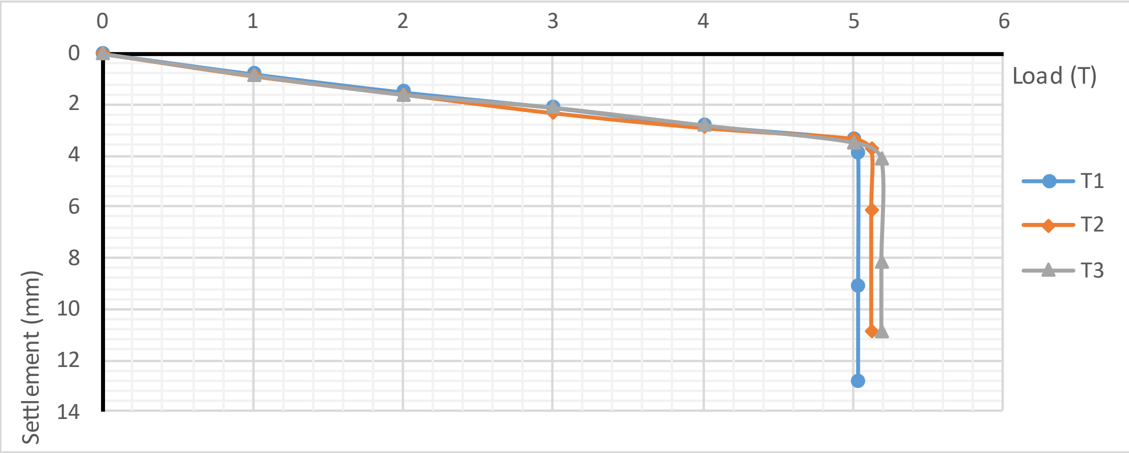

Fig. 8: Plate loading test result at Third R.L. level No. (3)

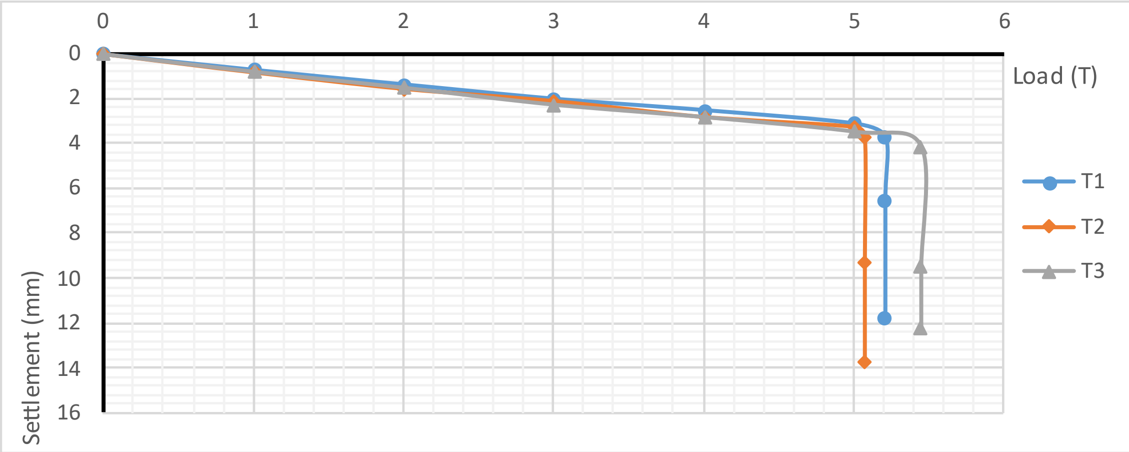

Fig. 9: Plate loading test result at Fourth R.L. level No. (4)

3.5 Fourth Replacement Layer Level

After placing the fourth replacement layer and reached to (D = -2.00m). It was noted in **Error! Reference source not found.**, the average ultimate bearing capacity increases 23%, then the excavation level. At test 1 the $q_{ult.}$ = 32.755 t/m^2 at Q_{max} = 5.208 ton, while at test 2 the q_{ult} = 31.908 t/m^2 for Q_{max} = 5.073 ton, and finally the q_{ult} = 34.256 t/m^2 at Q_{max} = 5.447 ton with averages of q_{ult} (average) = 32.973 t/m^2.

3.6 Fifth Replacement Layer Level

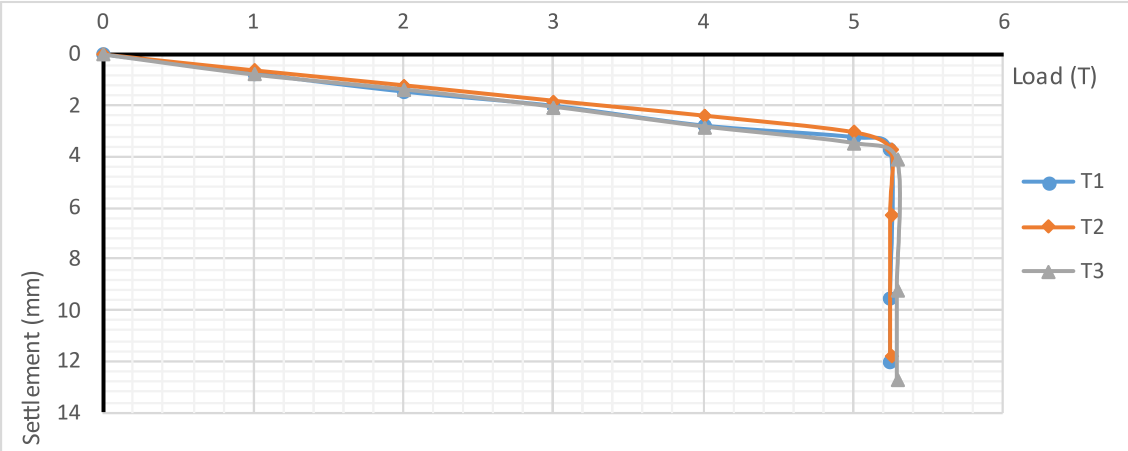

Fig. 10: Plate loading test result at Fifth R.L. level No. (5)

As illustrated in **Error! Reference source not found.**. After placing the fifth replacement layer and reached to (D = -1.75m). It was noted that the value of the average ultimate bearing capacity increases by 23.9%, proportional to the excavation level. At test 1 the $q_{ult.}$ = 32.964 t/m^2 at Q_{max} = 5.241 ton, while at test 2 the q_{ult} = 33.014 t/m^2 for Q_{max} = 5.249 ton, and finally the q_{ult} = 33.292 t/m^2 at Q_{max} = 5.293 ton with averages of q_{ult} (average) = 33.090 t/m^2.

3.7 Sixth Replacement Layer Level

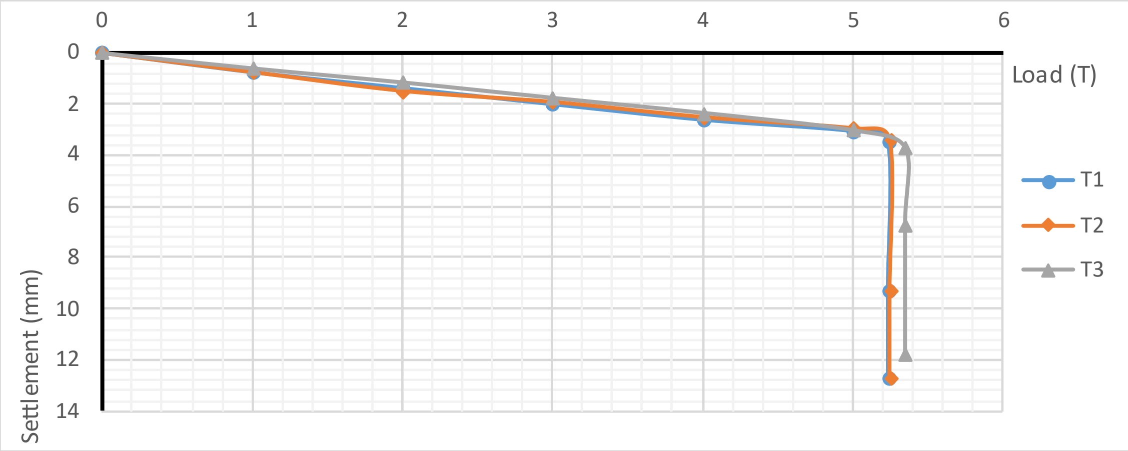

Fig. 11: Plate loading test result at Sixth R.L. level No. (6)

After placing the sixth replacement layer and reached to (D = -1.50m). The average of ultimate bearing capacity increases by 23.77% than that obtained from the result of excavation level. At test 1 the $q_{ult.}$ = 32.924 t/m^2 at Q_{max} = 5.235 ton, while at test 2 the q_{ult} = 33.017 t/m^2 for Q_{max} = 5.250 ton, and finally the q_{ult} = 33.620 t/m^2 at Q_{max} = 5.346 ton with averages of q_{ult} (average) = 33.187 t/m^2, **Error! Reference source not found.**.

3.8 Averages of Ultimate bearing Capacity

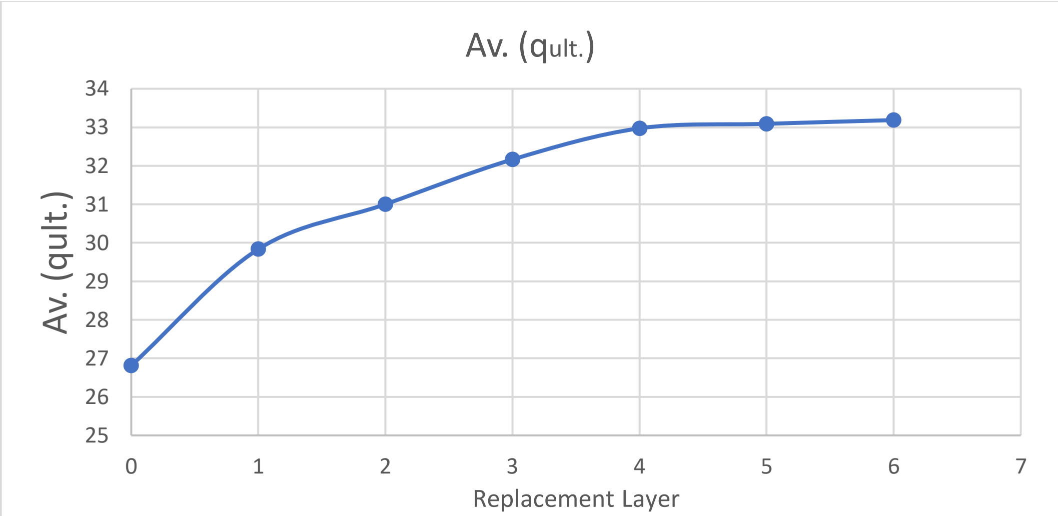

Fig. 12: Average (qult.) result at each layer

The ultimate bearing capacity increases by 11.3%, 15.6% and 20.0% after constructing the first, second and third replacement layer respectively. And 23.0% for the fourth replacement layer. Finally, a staidly increase is observed in the fifth and the sixth replacement layer recording 23.4% and 23.8% respectively, all these percentage were estimated from the natural soil as listed in Table 6, **Error! Reference source not found.**.

Table 6: Average ($q_{ult.}$) result at each layer

Soil Layers	AV. $q_{ult.}$ (t/m)	$q_{ult.}$ Increase (%)
Natural Soil	26.813	-
First	29.835	11.3
Second	31.002	15.6
Third	32.164	20.0
Fourth	32.973	23.0
Fifth	33.09	23.4
Sixth	33.187	23.8

IV. CONCLUSION

This research is using plate loading test to investigate the effect of replacement layers on the ultimate bearing capacity ($q_{ult.}$). These studies would help to better understand the relationship between replacement layer thickness and ultimate bearing capacity, and could lead to the development of improved design guidelines for replacement layer thickness.

According to the results obtained from plate loading tests at variant thickness of replacement layer, the following conclusion can be drawn the ultimate bearing capacity (q_{ult}) increased with the increasing of replacement layers thickness.

The results of this study have shown that the effect of replacement layer thickness on ultimate bearing capacity slightly after the fourth layer. in addition to that increasing replacement layer thickness beyond the fourth layer may be limited.

The replacement layers lead to the development of improve the design guide lines for constructions of foundation.

REFERENCES

[1] Ashraf, M.G., *"Bearing Capacity of Shallow Foundations on Non-Cohesive Soil"*, Journal of Geotechnical Eng., ASCE, Vol. 122, No. 2, pp. 167-168, (1997).

[2] Bowles, J. E., *"Foundation Analysis and Design"*, 5th Edition, McGraw-Hill, (2001).

[3] Coduto, D.P., Kitch, W.A., & Yeung, M.R., *"Geotechnical Engineering: Principles and Practices"*, Boston: Pearson, (2011).

[4] Das, B. M., *"Principles of Foundation Engineering"*, 8th Edition, Thomson Brooks/Cole, (2017).

[5] Egyptian Code of Soil Mechanics, *"Foundations Carrying Out and Designation"*, Part 2, 6th Edition, Laboratory Tests, Housing and Building National Research Center (HBRC), (2001).

[6] El-Kasaby, E.A., *"Soil Mechanics"*, Scientific Books House, Cairo, Egypt. (1993), (In Arabic language).

[7] Frankli, K., *"Pile Driving by Direct Displacement"*, Engineering, 208(5382), 566-567, (1969).

[8] Garber, M.; and Baker, R., *"Bearing Capacity by Variational Methods"*, Journal of Geotechnical Eng. Div., ASCE, No. 5, pp. 695-698, (1979).

[9] Hegazy, A.A., *"In-Situ and Laboratory Bearing Tests for Estimating Bearing Capacity of Shallow Footings Subjected To Inclined Loads"*, Ph. D. Thesis, Faculty of Engineering, Assuit University, Egypt, (1999).

[10] Mayerhof, G., *"Ground Engineering"*, John Wiley & Sons, (1967).

[11] Perkins, S.N., *"Bearing Capacity of Highly Frictional Material"* Geotechnical Testing Journal, Vol. 18, No. 4, pp. 450-462, (1995).

[12] Poulos, H. G., & Davis, E. H., *"Pile Foundation Analysis and Design"*, John Wiley & Sons, (1980).

[13] Reznik, Y.M., *"Rigid Plate Settlement on Soils with Varying Deformation Properties"*, Geotechnical Testing Jornal, ASTM, Vol. 18, No. 2, pp. 194-203, (1995).

[14] Terzaghi, K., & Peck, R. B., *"Soil Mechanics in Engineering Practice"*,2nd Edition, John Wiley & Sons, (1967).

[15] Tomlinson, M. J., *"Pile Design and Construction Practice"*, 5th Edition, Taylor & Francis, (2013).

[16] Tomlinson, M. J., *"The Bearing Capacity of Footings on Sands and Gravels"*, Proceedings of the 4th International Conference on Soil Mechanics and Foundation Engineering, London, England, 1, 169-190, (1971).

[17] Vesic, A. S., *"Analysis and Design of Shallow Foundations"*, John Wiley & Sons, (1973).

[18] Winterkorn, H.F., & Fang, H.-Y., *"Foundation Engineering Handbook"*, 3rd edition, Boca Raton, FL: CRC Press, (2006).

[19] El-Kasaby, El-Sayed A., et al. "Behavior of Square Footings Reinforced with Glass Fiber Bristles and Biaxial Geogrid." European Journal of Geotechnical Engineering, Vol..8, No.4, pp. 5-11, (2023).

[20] El-Kasaby, El-Sayed A., et al. "Enhancing Flexural Performance of GFRC Square Foundation Footings through Uniaxial Geogrid Reinforcement." International Journal of Civil Engineering and Structural Analysis, Vol..9, No.8, pp. 15-22, (2023)

International Journal of Advanced Engineering, Management and Science (IJAEMS)
Peer-Reviewed Journal
ISSN: 2454-1311 | Vol-10, Issue-2; Feb, 2024
Journal Home Page: https://ijaems.com/
DOI: https://dx.doi.org/10.22161/ijaems.102.4

Study the effect of Industrial Dairy, Textile, Leather and Paper Waste Water on the Engineering and Geotechnical Properties of Fine-Grained Soil

Elsayed A. El Kasaby, Alnos A. Eissa, Alaa F. Essa, Eman M. Hawari

Dep. of Civil Eng. Faculty of Engineering, Benha University, Egypt
E-mail: alaafoly1988@gmail.com
mergawieman@gmail.com

Received: 08 Jan 2024; Received in revised form: 12 Feb 2024; Accepted: 22 Feb 2024; Available online: 28 Feb 2024

***Abstract*— *Comprehend and forecasting the engineering characteristics of fine-grained soils is crucial for the practice of geotechnical engineering. Fine-grained soil contamination occurs on a daily basis as a result of industrial development and pipeline or reservoir leaks. Due to the influence of the surrounding condition, substantial damage occurs in the foundations of buildings. The presence of industrial wastewater in the soil contributes to a change in its physical, chemical and mechanical properties, and then negatively affects the foundations of various facilities. In addition to environmental issues such as groundwater contamination, the changing of the geotechnical qualities of polluted soil is a concern. As a result of the concentrations of pollutants resulting from the industrial businesses such as dairy products industry, spinning and weaving factories, paper factories and leather wastewater are extremely high in developing countries. Disposal of untreated industrial waste water is a common problem in these countries. This paper describes an experimental investigation that was conducted to explore the effect of four types of industrial wastewater; dairy (DW), textile (TW), leather (LW) and paper (PW) on the deformational behavior of fine-grained soil. Fine-grained soil was exposed to DW, TW, LW and PW for 2, 4, 6, 8, 12, and 16 months. Four remolded soil groups of samples are generated for this investigation and combined with the four types of industrial wastewater of constant moisture content (70%). The Atterberg limits, plasticity index, specific gravity, free swelling, optimal moisture content (OMC), and maximum dry density ($\gamma dmax$) of each mixture were calculated after 0, 2, 4, 6, 8, 12, and 16 months of mixing soil with industrial waste water. Comparisons were made between the results of four groups of samples.*

***Keywords*— Fine-grained soil. Contaminated soil. Industrial waste water. Geotechnical properties.**

I. INTRODUCTION

Soil pollution stemming from a variety of industrial wastewater byproducts stands as a significant geo-environmental concern, adversely affecting soil quality, groundwater, and the atmosphere. The acceleration of industrialization and urbanization has generated substantial quantities of both solid and liquid waste, consequently leading to extensive alterations in the geotechnical characteristics of soil due to the disposal of wastewater into the ground, as noted in reference [1-2-3]. Incidents of foundation and structural failures attributed to soil contamination and chemical spills have been documented in several reports [1, 2, 3, 4]. Extensive research has shown that various geotechnical properties of fine-grained soils can be influenced by both inorganic and organic contaminants typically present in industrial effluents [5, 6, 7]. To address the needs of diverse engineering applications, it is essential to thoroughly investigate and comprehend the interactions between soil and pollutants, as well as the repercussions of pollutants and industrial effluents on various geotechnical characteristics.

A comprehensive examination of the existing body of literature reveals that, to date, the primary emphasis has been on comprehending how pure chemicals affect commercial soils such as kaolinite and bentonite. There is comparatively limited research available regarding the effects of industrial effluents, especially on natural soils [8,9].

Industrial wastewater can contain hazardous substances that are relatively water-soluble, with examples including those originating from textile, dairy, and leather waste. The contamination of industrial wastewater poses significant risks to wildlife, including the poisoning of apex predators that consume organisms with accumulated wastewater in their tissues. This contamination can disrupt breeding patterns by making animals ill and unable to reproduce.

Despite comprehensive research on the geotechnical attributes of polluted fine-grained soils, there has been limited investigation into the impact of wastewater pollution on the geotechnical properties of such soils [11, 13].

Khan et al. (2017), Stalin et al. (2010), and Easa et al. (2002) have all conducted laboratory testing programs aimed at assessing the influence of wastewater contamination and its time effect on the geotechnical properties and behavior of fine-grained soil [1,6,8]. In Easa et al.'s (2010) study, samples of naturally contaminated groundwater sourced from household wastewater were obtained at the groundwater pumping level. The assessment involved the use of X-ray and conventional chemical testing to determine the concentration of toxins present in the groundwater [14]. The research findings suggest that residential wastewater is considered the predominant source of groundwater pollution due to its extremely hazardous and toxic chemical composition [15,16]. This contamination poses a substantial threat to public health. Additionally, a separate study highlighted the capacity of clay to expand as a result of fluctuations in water content, which can be induced by groundwater, leading to upward pressure on foundations. The expansion of clay and the resulting swelling pressure can result in substantial damage, including the cracking of walls, beams, and columns, particularly when the soil's swelling pressure exceeds the foundation load [17,18,19].

The thorough prediction of soil geotechnical parameters is a critical practice in geotechnical engineering, particularly in the presence of contamination [20]. Soil characteristics are altered as a result of ground pollution, Soil property changes cause a variety of geotechnical issues such as structural cracks, ground settlement, heaving of structures, slope instability, depletion of strength and deformation characteristics, changes in compaction characteristics, and so on.

Previously, the adequate attention of construction damages was attributed to many factors such as inadequate construction material, differential settlement, the destructive role of expansive and collapsing soil, etc. While, the effect of waste water on soils was taken as second or third reason of building and construction problems [8].

Recently, progressive increasing of constructions damage caused due to effect of waste water on soil was reported by engineers and investigations [21-24] So, engineers are concerned about the amount of damage caused by waste water to buildings, foundations, and soils.

On the other hand, if the chemical composition of the water in the pores of the clay is changed, the physical and mechanical properties of the clay are expected to change. Thus, the pore fluid type and composition strongly affect the engineering behaviour of most soils especially clayey soils [25-27].

Furthermore, several investigations have shown that, the pollution of soil has important influence on the physical and mechanical properties of clay [28, 29].

Hence, modern building necessitates not only a prior examination of the foundation material, but also a complete understanding of the processes that cause the changing of soil qualities over the life of the structures supported by it.

Kirov (1989) observed the influence of wastewater on deformation behavior of clayey soil, He found that soils interacting with a solution of detergents undergo a large amount of deformation. Srivastava et al. (1992) observed increase in consistency limit, permeability and coefficient of compression and decrease in shear strength and bearing capacity of a soil specimen permeated with fertilizer plant effluent[29,30].This is due to decrease in cation content and increase in hardness of leaching water after interaction Decrease of liquid limit and plasticity index of montmorillonite soil due to addition of pharmaceutical effluent to the soil has been found due to decrease of dielectric constant by contamination. Yaji et al. (1996) have investigated the influence of sugar mill liquid wastes on the behavior of shedi soil. At large percentages of sugar mill liquid wastes, shear strength decreases [31].

Generally, industrial wastes contain acids, alkalis, sulphates, salts, urea (amides), and oil pollutants, which cause changes in the physicochemical, mechanical and geotechnical properties of the soil. Several case studies of soil contamination with industrial pollutants and their impact on soil geotechnical behavior are presented below. El-Kasaby, A., Easa, A.F (2023) and El-Kasaby, A., Easa, E.M (2023).

The Problem Scope

The danger arises from industrial wastewater, which poses a real threat to the soil, groundwater, and the mechanical behavior of fine-grained soil. The effect of industrial spread throughout Egypt on fine-grained soil has not been studied, engh, the researchers try to identify the properties of contaminated soil to avoid potential risks and also to use contaminated soil beneficially in civil engineering projects.

II. EXPERIMENTAL STUDY

According to a comprehensive review of the literature, studies on the influence of industrial wastewater of dairy, textile, leather and paper effluent on natural soils are infrequent or scarce. The wastewater used in this case originated from four separate sources. The first originated from Dairy factory in Minya Governorate, the second from Textile factory in Obour City, Qalyubia Governorate. The third came from tanneries in Ain Al-Sirah, Cairo, and finally from a paper factory, Islamic company in Quesna, Menoufia Governorate These potentially hazardous wastewaters, whose environmental consequences necessitate continuing monitoring, were collected after solids deposition but before treatment. According to a critical review of the literature, considering the foregoing, the four types of industrial wastewaters; dairy, textile, leather and paper wastewater, which are referred to as DW, TW, LW, and PW respectively, were chosen for the current investigation. Natural fine-grained soil used in this research was obtained in a natural phase from a soil excavation site for the construction of a residential building in the village of El-Kom Al-Ahmar, Shibin El-Qanater, Qalyubia governorate, Egypt, **Fig. (1).**

The various effluents in "as collected form" as well as the outflow from the experimental setup, i.e., pH, alkalinity, total solids, total dissolved solids (TDS), total volatile solids (TVS), chloride, and biochemical oxygen demand (BOD) were estimated to be characterized by the effluent parameters. The metrics are complete and adequate for describing the effluent and understanding its impact on the specified soils. The parameter analysis method was carried out in accordance with Standard Methods. The properties of dairy (DW), textile (TW), leather tanneries (LW) and paper (PW) effluent are listed in **Tables (1), (2), (3) and (4)**. Representative soil samples from the chosen regions were collected in 150 kilograms airtight polythene bags, transported to the lab, and stored in airtight containers under normal conditions and keep at laboratory temperature until usage.

Fig.1: Site of soil sample

Table. 1: Physical properties of wastewater (DW, TW, LW and PW)

Properties	Value			
	DW	TW	LW	PW
Color	light yellow	greenish grey	translucent	grey
Temperature (C)	22	24	21	23
PH (Value)	10.3	11.80	9.9	11.4
Total Suspended Solids (TSS), (mg/liter)	2772	2684	1913	2314

Table. (2). Organic properties of wastewater (DW, TW, LW and PW)

Properties	Value (mg/liter)			
	DW	TW	LW	PW
Volatile Suspended Solids (VSS)	985	1217	1683	1122
Biological Oxygen Demand (BOD)	686	912	821	1308
Total organic carbon (TOD)	284	448	336	677
Chemical Oxygen Demand (COD)	4513	3876	2757	6881
Oil &Grease	174	266	378	125
Phenol	8.5	9.7	11.5	9.2
Detergents	17.5	22.4	11.7	25,7
Pesticides	2.4	7.5	9.2	6.4

Table. (3). Chemical properties of wastewater (DW, TW, LW and PW)

Properties	Value (mg/liter)			
	DW	TW	LW	PW
Chloride (Cl-)	2942	1968	3764	1997
Sulfate (SO42-)	757	3827	2843	1719
Alkalinity (CaCO3)	176	868	473	574
Ammonia (NH3-N)	65	162	267	157
Phosphate (SO43-)	4.5	17.7	10.2	19.5

Table. (4). Chemical minerals of the samples (DW, TW, LW and PW).

Properties	Value (mg/liter)			
	DW	TW	LW	PW
Aluminum	0.20	0.40	0.25	0.15
Chromium	1.05	1.80	1.55	2.15
Copper	0.05	1.70	2.4	1.8
Iron	2.45	0.55	1.65	1.4
Lead	0.11	1.25	3.65	0.75
Manganese	1.80	7.2	11.6	9.1
Nickel	0.02	2.73	6.80	4.55
Borne	0.06	4.82	2.80	2.76
Selenium	0.12	0.58	0.57	0.75
Fluoride	10.85	8.73	4.65	12.52
Zinc	0.00	3.70	5.60	7.25
Arsenic	0.07	0.11	0.17	0.08
Cyanide	0.01	1.87	2.10	2.23
Mercury	0.001	0.057	0.057	0.068
Cadmium	0.03	0.063	0.088	0.075

III. EXPERIMENTAL SET-UP AND SOIL SAMPLE PREPARATION

Experimental program includes four groups, each with six contaminated soils (TW or DW or LW or PW) in addition to natural soil for comparison. These groups were constructed after mixing and according to the timeline. Each set of soils under consideration was generated and used for the following purposes:

1. Samples were collected from the site and stored in the laboratory.
2. Since each effluent was utilized to investigate how industrial waste materials affected the mechanical and geometric qualities of natural soil at different ages. As a result, only four sets of polluted soils were used for research purposes. Soil tests were conducted 2, 4, 6, 8, 12, and 16 months after the date the contaminant was added to the soil.
3. Total of 25 samples were used to study the influence of four effluents (TW, DW, LW and PW) on natural soil (S1). A 10-kilogram soil sample is manually mixed with effluents at their water content (70%) before being transported.

Scanning electron microscopes (SEM) and X-ray diffraction (XRD) were also utilized to examine the mineral compositions of natural and polluted samples [DW6, TW6, LW6 and PW6] that was, 16 months after the date of adding the pollutant. These techniques are available at Egyptian Mineral Resources Authority's Central Laboratories Sector's. The experimental program was developed in order to determine the swelling behavior of the tested soils in addition to tests for liquid limit (L.L), plastic limit (P.L), shrinkage limit (S.L), specific gravity (GS), and finally the standard Proctor test.

IV. RESULTS AND DISCUSSION

4.1 Physical Properties

4.1.1 Atterberg's limits

Atterberg's limits contains of liquid limit (L.L), plastic limit (P.L) and shrinkage limit (S.L). The obtained results of L.L, P.L and S.L, **Fig. (5), (6) and (7),** plasticity index (PI=LL-PL) **Fig. (8),** in addition to that **Table (5)** contains results of Atterberg's limits and specific gravity (GS) **Fig. (9).** According to these findings and the unified soil classification system (USCS) as listed in Table 5.

Based on the liquid limit results:

- Values of the liquid limit (for all contaminated soils) decrease as the duration of the contamination effect increases. But soil exposed to industrial wastewater from paper is more affected than soils exposed to other pollutants.
- There was a disturbance in the liquid limit (L.L) values, with the increase of contamination effect period for soil that had been contaminated by textile wastewater.
- The natural soil's plastic limit (PL) value was 33%. While the relative levels of contamination (PL) of soil with textile wastewater (TW) are ranged from 34.5% to 33%. The PL of soil contaminated with dairy effluent (DW) ranged from 32% to 27%, the PL of soil contaminated with leather wastewater (LW) ranged from 33% to 29% but the PL of soil contaminated paper wastewater (PW) ranged from 35% to 41%.

According to the plastic limit results:

- For soil that had been contaminated by Dairy (DW) and leather wastewater (LW), the plastic limit values were decrease with the increase of contamination effect period.
- There was a disturbance in the Plastic limit (P.L) values, with the increase of contamination effect period for soil that had been contaminated by textile wastewater.
- The soil that had been contaminated by paper wastewater (PW), the plastic limit values were increase with the increase of contamination effect period.
- The shrinkage limit (SL) of natural soil was 18%. While the (SL) values of soil that has been contaminated with textile wastewater (TW) range from 19.2% to 20.5%. The (SL) results of soil contaminated with dairy effluent (DW) were 19% to 21%, respectively. the SL of soil contaminated with leather wastewater (LW) ranged from 19% to 25% but the SL of soil contaminated paper wastewater (PW) ranged from 21% to 26%.

Related to the shrinkage limit (SL) results:

- the shrinkage limit (S.L) values increase with the increase in the duration of the pollution effect until 6 months have passed, then at effect period 8, 12 and 16 months, the samples were broken, for soil that had been contaminated by Dairy (DW) and textile wastewater (TW).
- For soil that had been contaminated by leather waste water (LW), the shrinkage limit (S.L) values increase with the increase in the duration of the pollution Up to 16 months.
- the shrinkage limit (S.L) values increase with the increase in the duration of the pollution effect until 8

months have passed, then at effect period 12 and 16 months, the samples were broken.

- The plasticity index (PI) of natural soil was 41%. While the (PI) values of soil that has been contaminated with textile wastewater (TW) range from 27.5% to 30%. The (PI) results of soil contaminated with dairy effluent (DW) were 36.5% to 35%. The PI of soil contaminated with leather wastewater (LW) ranged from 38% to 33% but the PI of soil contaminated paper wastewater (PW) ranged from 29% to 16%.
- According to the results of plasticity index (PI) for soil that had been contaminated by Dairy (DW) it was decrease with the increase of contamination effect period until 2months have passed, then at effect period 4, 6,8,12 and 16 months, there was stability in the values of the plasticity index.
- For soil that had been contaminated by (TW) and (LW) the plasticity index (PI) values were decrease with the increase of contamination effect period until 6months have passed, then at effect period 8,12 and 16 months, after that they increased slightly.
- The soil contaminated by paper waste water (PW) values were decrease with the increase of contamination effect period.

Table. (5). The results of Atterberg's limit for natural soil and contaminated soil with TW, DW, LW and PW at different time (Months).

Effect Period		LL %	PL %	PI %	SL %
O Si		74	33	41	18
2 Months	TW (%)	62	34.5	27.5	19.2
	DW (%)	66.5	32	36.5	19
	LW (%)	71	33	38	19
	PW (%)	64	35	29	21
4 Months	TW (%)	62	35	27	20.5
	DW (%)	65	30	35	20
	LW (%)	68	32	36	20
	PW (%)	62	36	26	23
6 Months	TW (%)	62.5	35.5	27	20.5
	DW (%)	64	29	35	21
	LW (%)	65	30	35	21
	PW (%)	60	37	23	25
8 Months	TW (%)	63	35	28	Broken
	DW (%)	63	28	35	Broken
	LW (%)	63	30	33	23
	PW (%)	59	38	21	26
12 Months	TW (%)	63	34	29	Broken
	DW (%)	62.5	27	35	Broken
	LW (%)	62.5	29	33.5	24
	PW (%)	58	39	19	Broken
16 Months	TW (%)	63	33	30	Broken
	DW (%)	62.5	27	35	Broken
	LW (%)	62.4	29	33	25
	PW (%)	57	41	16	Broken

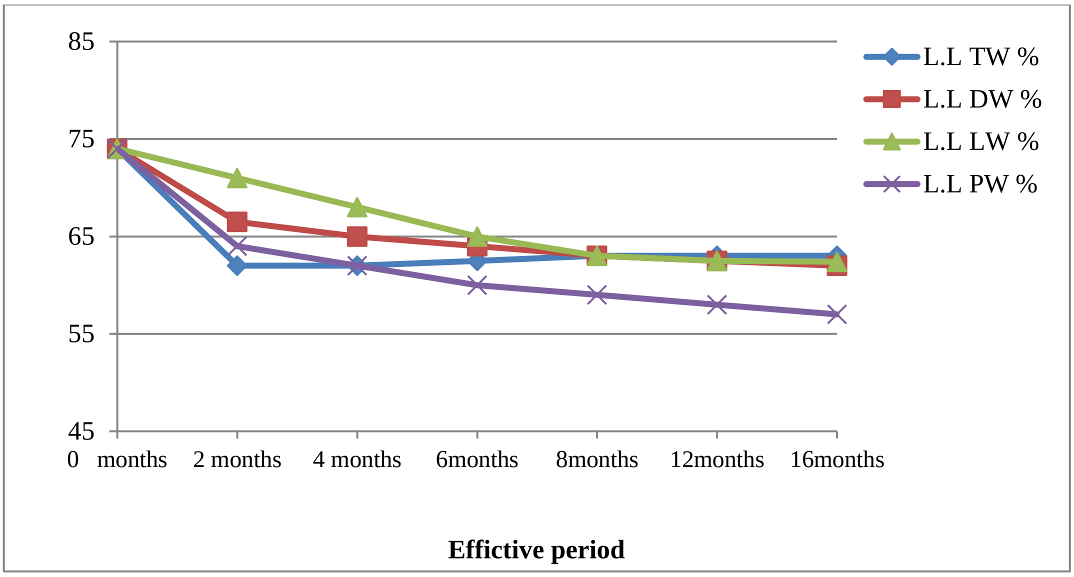

Fig. (5). Comparison between the liquid Limit results with ageing of exposure for TW, DW, LW and PW.

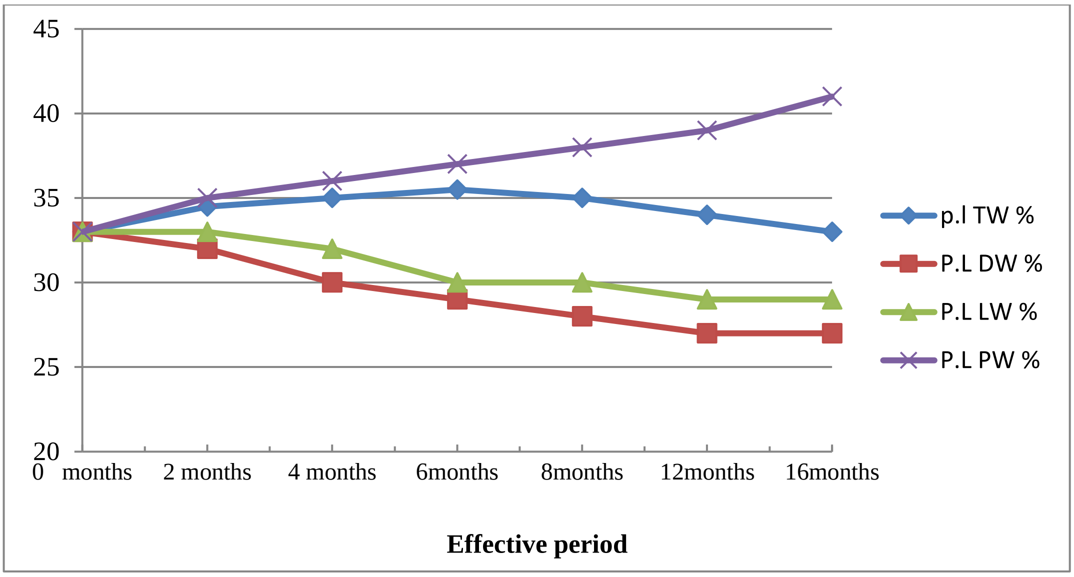

Fig. (6). Comparison between the plastic Limit results with ageing of exposure for TW, DW, LW and PW.

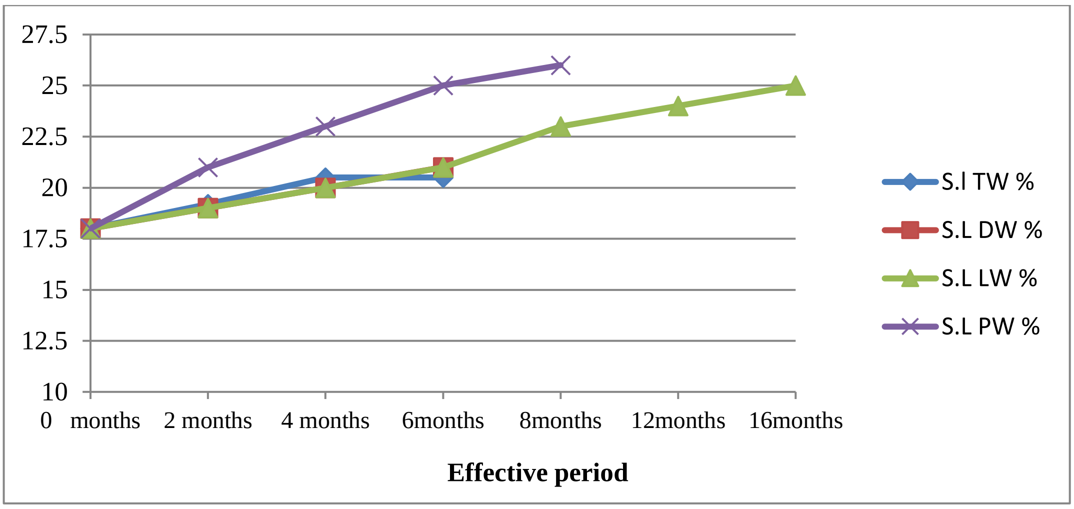

Fig. (7). Comparison between the (SL) values with ageing of exposure for TW, DW, LW and PW.

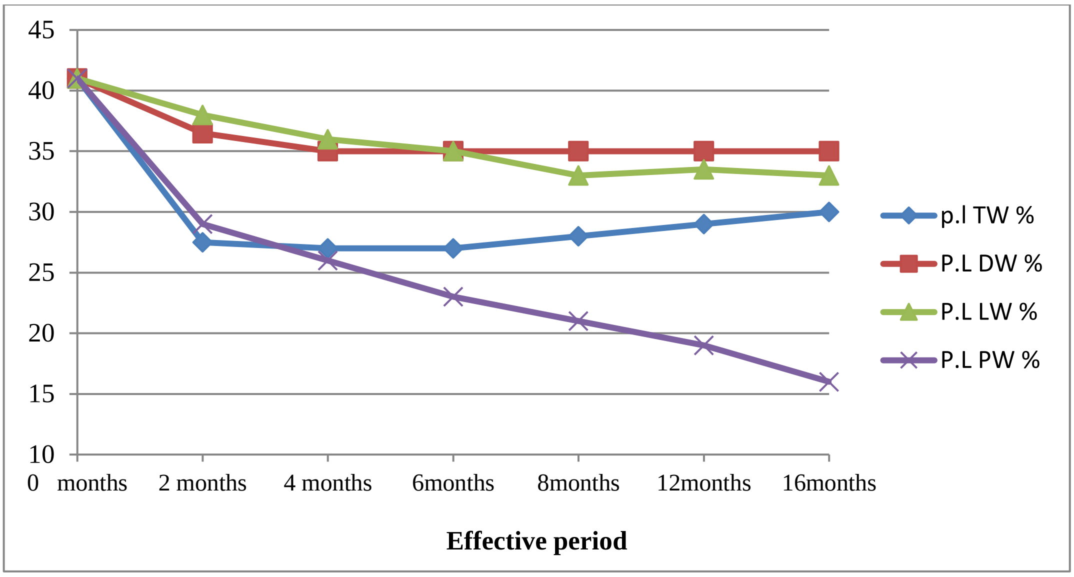

Fig. (8). Comparison between the plasticity index values with ageing of exposure for TW, DW, LW and PW.

According to these findings and the unified soil classification system (USCS) as listed in **Table (6):**

- The natural soil, which is categorized as silty clay with high plasticity (CH-MH).
- The contaminated soil samples for textile wastewater (TW) and industrial paper wastewater (PW) were classified as silt with high plasticity (MH) in the effect periods 2, 4, 6 and 8 months, but at 12 and 16 months, the (PW) classified as silt with low plasticity (ML) based on the impact of industrial wastewater as per the unified classification system (USCS).
- According to the effect of dairy wastewater (DW) was classified as clay with high plasticity (CH), while soil samples contaminated with leather wastewater (LW) was classified as (CH-MH) in 2 months and 4 months, and classified as clay with high plasticity (TH) in the effect periods 6, 8, 12 and 16 months.

Table (6). Classification of contaminated soils according to the unified soil classification system (USCS)

Effective Period	0 Months (S1)	2 months	4 months	6 months	8 months	12 months	16 months
TW	CH-MH	MH	MH	MH	MH	MH	MH
DW	CH-MH	CH	CH	CH	CH	CH	CH
LW	CH-MH	CH-MH	CH-MH	CH	CH	CH	CH
PW	CH-MH	MH	MH	MH	MH	ML	ML

- The specific gravity (GS) of natural soil was 2.67. While the specific gravity (GS) values of soil that has been contaminated with textile wastewater (TW) range from 2.65 to 2.6, (GS) values for soil contaminated with dairy effluent (DW) were 2.6 to 2.565, (GS) values for soil contaminated with leather wastewater (LW) range from 2.656 to 2.6 and finally (GS) values for soil contaminated with paper wastewater (PW) range from 2.65 to 2.58, **Table (7).**

According to the specific gravity (GS) results:

- For all contaminated soil with the different industrial waste water the (GS) values were decrease with the increase of contamination effect period. But soil exposed to industrial wastewater from dairy (DW) is more affected than soils exposed to other pollutants.

Table (7). The results of specific gravity for natural and contaminated soil with TW, DW, LW and PW at different times (months)

Effective Period	0 months	2 months	4 months	6 months	8 months	12 months	16 months
GS TW	2.67	2.65	2.635	2.63	2.61	2.61	2.6
GS DW	2.67	2.6	2.6	2.58	2.577	2.57	2.565
GS LW	2.67	2.656	2.65	2.644	2.634	2.6	2.6
GS PW	2.67	2.65	2.63	2.62	2.6	2.585	2.58

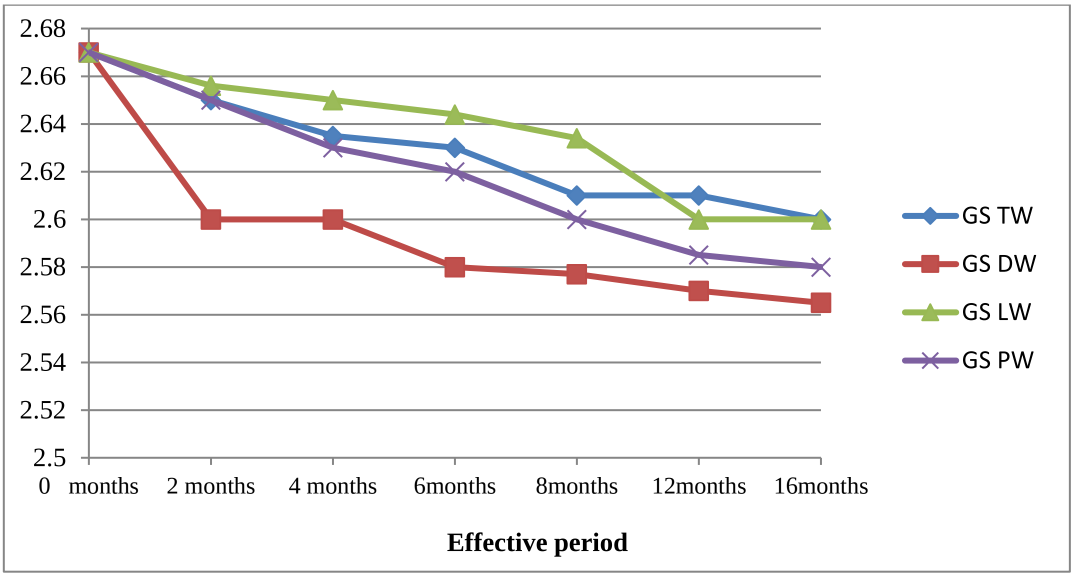

Fig. (9). Comparison between the specific gravity (GS) values with ageing of exposure for TW, DW, LW and PW

4.1.2 Free Swell Results

- Based on the free swelling (F.S) results obtained from the soil samples under study **Table (8),** the results showed that S1 (natural soil) was (60%), for soil contaminated with textile wastewater (TW) after (16months) from contamination was (79.5%) ,the results of the Free Swell (F.S) for soil contaminated with dairy effluent (DW) was (78%) and the results of the Free Swell (F.S) for soil with paper wastewater (PW) was (85%), on the other hand the Free Swell (F.S) value for soil contaminated with leather wastewater (LW) after 16 months was (40%) , **Fig. (10)**.
- For the soils (DW), (TW) and (PW) the (F.S) values were increase with the increase of contamination effect period, but for soil contaminated with Leather tanneries wastewater (LW), the free swell (F.S) values were decrease with the increase of contamination effect period.
- The soil exposed to industrial wastewater from paper is more affected than soils exposed to other pollutants.

Table (8). The results of (F.S) for natural and contaminated soil with TW, DW, LW and PW at the effective period

Effective Period	0 months(S1)	2 months	4 months	6 months	8 months	12 months	16 months
F.S TW%	60	70	72	75	76.5	77.5	79.5
F.SDW%	60	65	72.5	75	76	78	78
F.S LW%	60	55	50	43.5	43	40	40
F.S PW%	60	65	70	75	80	85	85

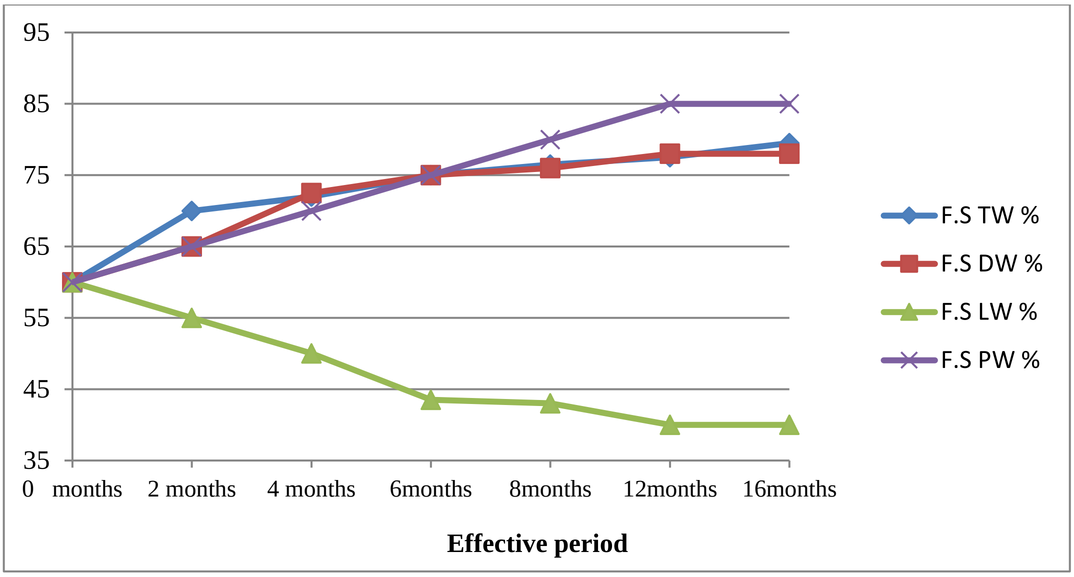

Fig. (10). Comparison between the FS values with ageing of exposure for TW, DW, LW and PW.

4.2 Compaction Outcomes

The compaction parameters (γdmax) and OMC are estimated for the natural soil and contaminated soils at different dates are shown in **Figs. (11) and (12).** Based on the results of the compaction test using the standard proctor apparatus. It is clear from **Table (9),** which includes the compaction findings as maximum dry density (γdmax) and optimum moisture content (OMC), that:

- The optimum moisture content (O.M.C.) and maximum dry density (γ_{dmax}) of natural soil (S1) were 20% and 1.70 gm/cm3, respectively, while these values ranged from 20.5% to 22.3% and 1.65 to 1.6 gm/cm3 for soil that had been contaminated TW. When soil was contaminated with DW effluent, the O.M.C. and dry density were, respectively, 22.5% to 24% and 1.61 to 1.53 gm/cm3.In another hand soil that had been contaminated LW waste water the (OMC) and (γdmax) values were, respectively, 21% to 25% and 1,65 to 1,52 gm/cm3 when soil was contaminated with (PW) the O.M.C. and dry density were, respectively, 22% to 26% and 1,63 to 1.46 gm/cm3
- The (γdmax) of all contaminated soils was lower than that of the natural soil. The (γdmax) of (PW) contaminated soil is the lowest, **Fig. (11)**.
- Optimum moisture content (OMC%) values increase of contamination effect period for all contaminated soils (TW), (DW), (LW) and (PW)
- For all contaminated soil with the different industrial waste water the maximum dry density (γ_{dmax}) values decrease with the increase of contamination effect period. But soil exposed to industrial wastewater from paper (PW) was the most affected

Table (9). Compaction out comes for the studied soils

Sample No	Sample No	O.M.C, %	γdmax., gm/cm3
Natural Soil	S1	20	1.7
Contaminated soil with TW	TW1 (2 month)	20.5	1.65
	TW2 (4 month)	21	1.64
	TW3 (6 month)	21.5	1.62
	TW4 (8 month)	21.75	1.61
	TW5(12 month)	22	1.6
	TW6(16 month)	22.3	1.6
	DW1 (2 month)	22.5	1.61
	DW2 (4 month)	22.75	1.6

Contaminated soil with DW	DW3 (6 month)	23	1.58
	DW4 (8 month)	23.5	1.57
	DW5 (12 month)	24	1.54
	DW6 (16 month)	24	1.53
Contaminated soil with LW	LW1 (2 month)	21	1.65
	LW2 (4 month)	22.25	1.63
	LW3 (6 month)	23	1.62
	LW4 (8 month)	24	1.6
	LW5 (12 month)	24.25	1.55
	LW6 (16 month)	25	1.52
Contaminated soil with PW	PW1 (2 month)	22	1.63
	PW2 (4 month)	22.5	1.6
	PW3 (6 month)	24	1.56
	PW4 (8 month)	24.75	1.55
	PW5 (12 month)	25	1.5
	PW6 (16 month)	26	1.46

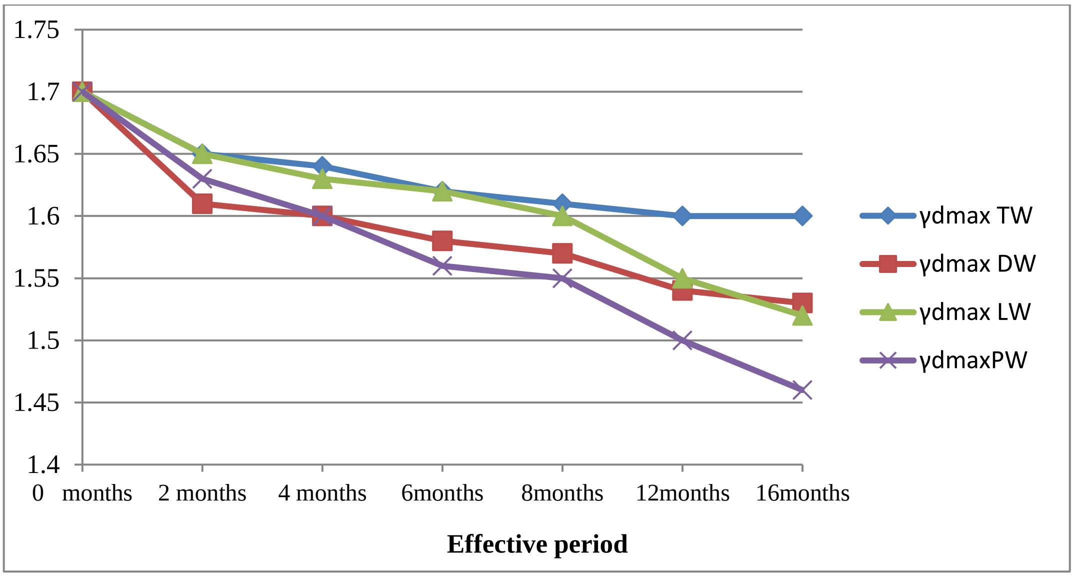

Fig. (11). Comparison between the (γdmax) results with ageing of exposure for TW, DW, LW and PW

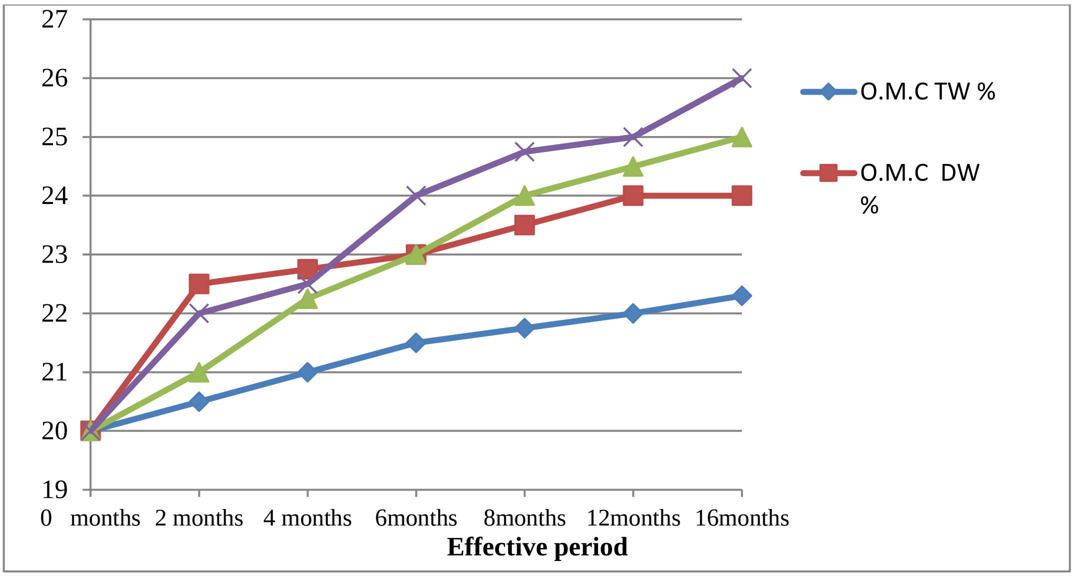

Fig. (12). Comparison between the (OMC) results with ageing of exposure for TW, DW, LW and PW

4.3 Chemical Analysis

4.3.1 Summary of Chemical Analysis of Soil

The chemical analysis of the natural soil sample S1 and the contaminated soils samples after 16 months from contamination for all contaminated soils (TW), (DW), (LW) and (PW) were carried out in National Research Center in Giza Governorate. **Table (10)** and **Fig. (13)** display the chemical analysis results, while **Fig. (13)** lists the major oxides for comparison between the values based on the chemical analysis.

- The presence of industrial wastewater can lead to an increase in certain chemical oxides. But soil exposed to industrial wastewater from paper (PW) was the most affected. It includes a high percentage of Alumina Oxide (Al2O3), Iron oxide (Fe2O3), and Titanium oxide (TiO2), in soil sample.
- Some chemical oxides in soil samples are decreased due to the contamination by paper industrial wastewater it contains the lowest percentage of Silicon oxide (SiO2), in soil sample.
- Some oxides are slightly decreased or increased.
- The above results of chemical oxides analysis agreed with the previous study by El-Kasaby, A., Easa, A.F (2023) and El-Kasaby, A., Easa, E.M (2023).

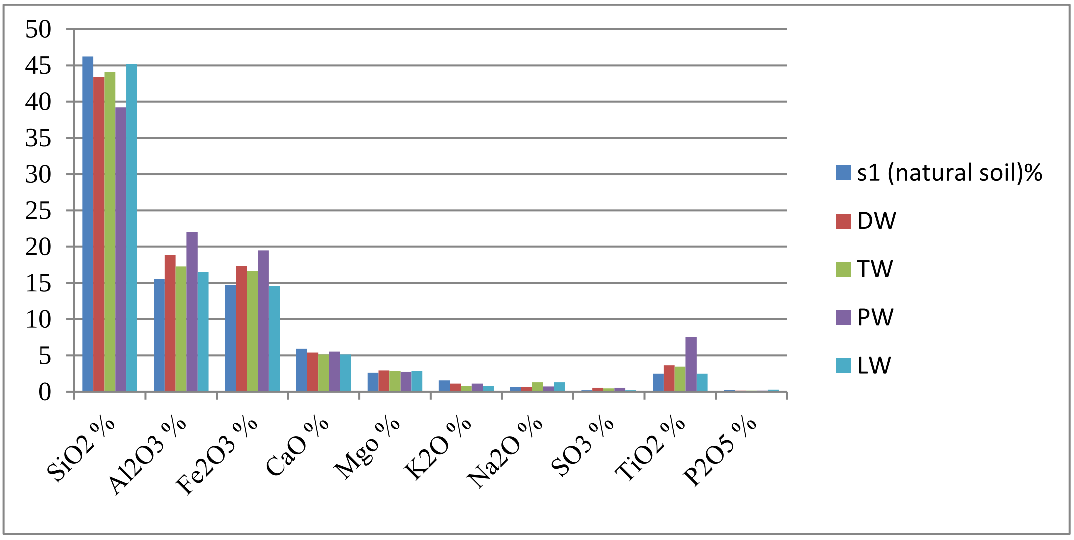

Fig. (13). Comparison between the Major Oxides in (S1) and the studied soils (DW), (TW), (LW) and (PW).

Table (10). Chemical analysis results for natural soil S1and all contaminated soils DW, TW, LW, PW

Oxide Content %	Soil Samples				
	Natural soil (S1)	(TW)	(DW)	(PW)	(LW)
SiO2	46.2	44.1	43.4	39.2	45.2
Al2O3	15.5	17.25	18.4	22.0	16.5
Fe2O3	14.70	16.60	17.3	19.5	14.60
CaO	5.92	5.14	5.4	5.54	5.14
Mgo	2.64	2.84	2.94	2.74	2.84
K2O	1.54	0.80	1.1	1.1	0.80
Na2O	0.65	1.30	0.68	0.74	1.30
SO3	0.19	0.45	0.55	0.53	0.18
TiO2	2.47	3.48	3.64	7.5	2.48
P2O5	0.26	0.14	0.13	0.15	0.27
MnO	0.23	0.45	0.44	0.41	0.24
SrO	0.05	0.04	0.06	0.08	0.04
ZrO2	0.05	0.05	0.06	0.07	0.05
Cr2O3	0.05	0.04	_	_	0.04
BaO	0.06	0.02	0.025	0.02	0.07
CO3O4	-	-	0.04	0.04	-
Nb2O5	0.01	0.03	0.02	0.05	0.03
LOi	9.35	6.32	5.39	9.3	9.49
Cl-	0.04	0.70	0.80	0.85	0.13

Where,

SiO_2	Silicon Oxide	MnO	Manganese Oxide
Al_2O_3	Alumina Oxide	SrO	Strontium Oxide
Fe_2O_3	Iron Oxide	ZrO_2	Zirconium Oxide
CaO	Calcium Oxide	Cr_2O_3	Chromium Oxide
Mgo	Magnesium Oxide	BaO	Barium Oxide
K_2O	Potassium Oxide	CO_3O_4	Cobalt Oxide
Na_2O	Sodium Oxide	Nb_2O_5	Nickel Oxide
SO_3	Sulphur tri Oxide	LOi	Loss of ignition
TiO_2	Titanium Oxide	Cl^-	Chloride
P_2O_5	Phosphorus Oxide		

4.3.2 Mineralogical Analysis of the Tested Soil

At Giza Governorate's National Research Centre, an X-ray diffraction analysis of four soil samples natural soil sample s1 and contaminated soil samples TW, DW, LW and PW was carried out. By using X-ray diffraction (XRD) and X-ray fluorescence spectroscopy (XRF), The X-ray diffraction patterns of S1, TW, DW, LW and PW, **Table (11)** presents the calculated mineral percentages.

Table (11). XRD semi-quantitative percentages results.

Sample No.	Quartz	Calcite	Kaolinite	Ellite	Montmorillonite
Natural soil	8.8	6.8	20.8	32.6	31
TW	8.67	5.8	23.4	39.25	22.88
DW	9.38	5.5	22.85	38.77	23.5
LW	10.4	5.9	24.2	39.8	20
PW	9.7	5.2	23.3	38.8	23

4.3.3 Scanning Electron microscopy Investigations (SEM)

The particle structure of the soils and wastewater was compared using scanning electron microscope (SEM) research. **Fig. (14), (15), (16), (17) and (18)** show the morphology of the tested soils. The primary structure of the current study's main structure usually contains the chemical elements silicon and aluminum, which are shown to have prominent peaks in the analysis. Figure 14, which displays the micrographs of natural soil devoid of wastewater, displays scanning electron micrographs of uncontaminated natural soil. The unique characteristics of natural soil, such as its high clay content, are highlighted by the stark variations in soil micrographs of natural soil before contamination. When comparing the micrographs in **Fig. (15), (16) ,(17) and (18)** it is clear how Dairy, Textile, leather and paper wastewater affects natural soil. When compared to natural soil, the microstructure of the contaminated soil particles was looser, more porous, and had a different surface shape. Sulphate activity causes disaggregation and the removal/washing out of constituents, strengthening the voids in some areas while causing aggregation and changes in the surface texture of the soil mass in other areas. The presence of clay is to blame for this.

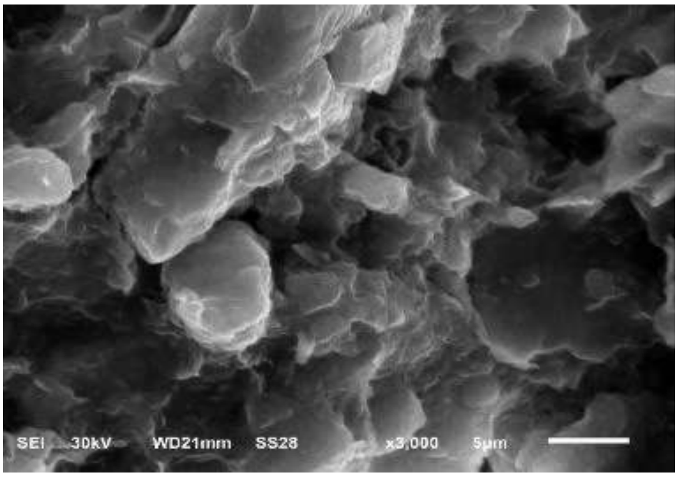

Fig. (14). SEM micrograph of natural soil before artificial contamination with wastewaters

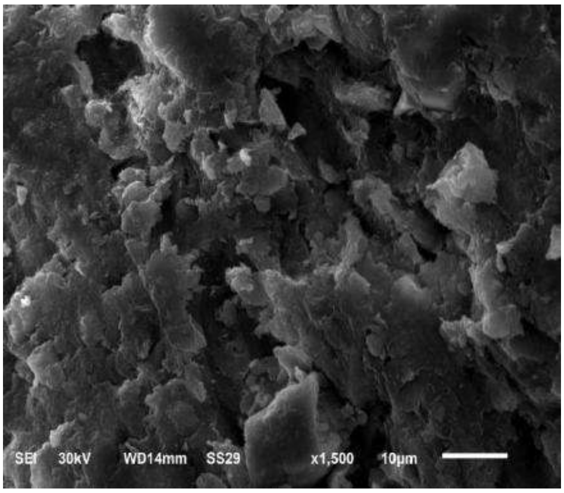

Fig.(15). SEM micrograph of natural soil after 16 months from contamination with wastewaters (DW)

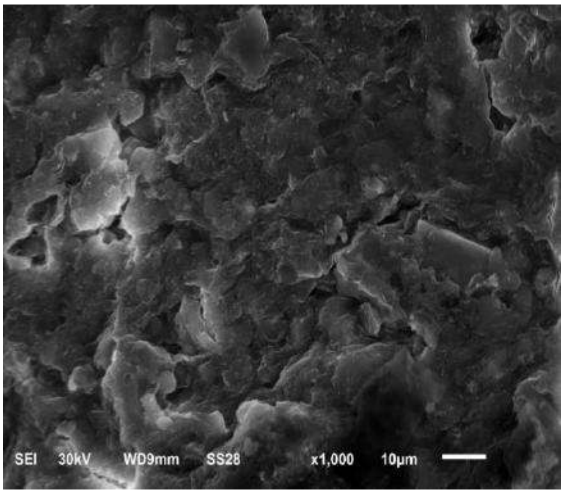

Fig. (16). SEM micrograph of natural soil after 16 months from contamination with wastewaters (TW)

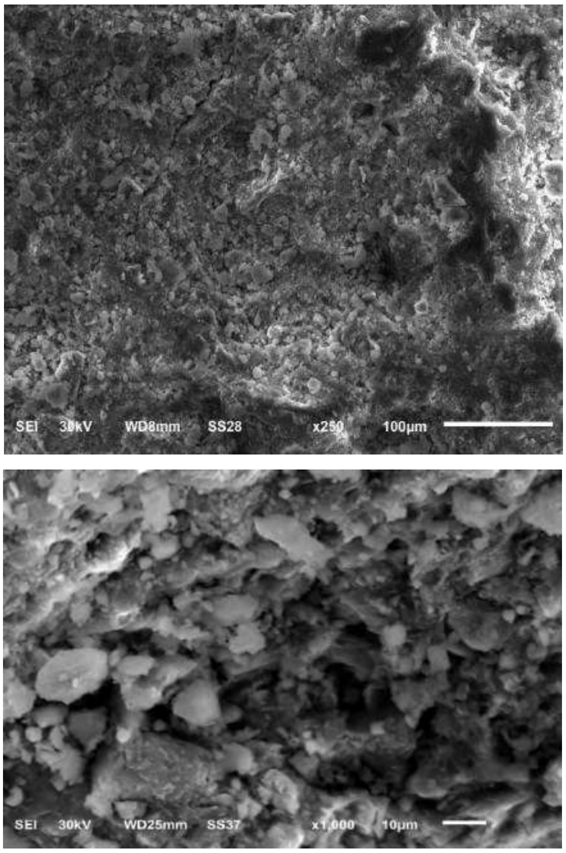

Fig. (17). SEM micrograph of natural soil after 16 months from contamination with wastewaters (LW)

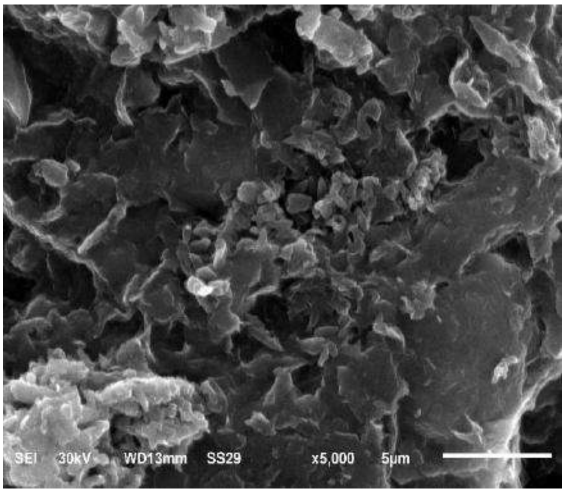

Fig. (18). SEM micrograph of natural soil after 16 months from contamination with wastewaters (PW)

V. CONCLUSION

According to Laboratory studies on these soil samples, the following can be drawn as:

1. It has been suggested that the geotechnical properties of fine-grained soil promote the degradation of dairy and textile products, perhaps posing threats to the site's current construction.
2. Values of the liquid limit (L.L.) decrease as the duration of the contamination effect increases. For all contaminated soils but soil exposed to industrial wastewater from paper is more affected than soils exposed to other pollutants.
3. There was a disturbance in the Plastic limit (P.L) values, with the increase of contamination effect period for soil that had been contaminated by textile wastewater.
4. For soil that had been contaminated by Dairy (DW) and leather wastewater (LW), the plastic limit values were decrease with the increase of contamination effect period.
5. There was a disturbance in the Plastic limit (P.L) values, with the increase of contamination effect period for soil that had been contaminated by textile wastewater.
6. The soil that had been contaminated by paper wastewater (PW), the plastic limit values were increase with the increase of contamination effect period.
7. the shrinkage limit (S.L) values increase with the increase in the duration of the pollution effect until 6 months have passed, then at effect period 8, 12 and 16 months, the samples were broken, for soil that had been contaminated by Dairy (DW) and textile wastewater (TW).
8. For soil that had been contaminated by leather waste water (LW), the shrinkage limit (S.L) values increase with the increase in the duration of the pollution Up to 16 months.
9. The shrinkage limit (S.L) values increase with the increase in the duration of the pollution effect until 8 months have passed, then at effect period 12 and 16 months, the samples were broken.
10. According to the results of plasticity index (PI) for soil that had been contaminated by Dairy (DW) it was decrease with the increase of contamination effect period until 2months have passed, then at effect period 4, 6,8,12 and 16 months, there was stability in the values of the plasticity index.
11. For soil that had been contaminated by (TW) and (LW) the plasticity index (PI) values were decrease with the increase of contamination effect period until 6months have passed, then at effect period 8,12 and 16 months, after that they increased slightly.
12. The soil contaminated by paper waste water (PW), the (PI) values were decrease with the increase of contamination effect period.

13. The natural soil, which is categorized as silty clay with high plasticity (CH-MH). The contaminated soil samples for (TW) and (PW) were classified as Silt with high plasticity (MH) after the effect periods 2, 4, 6 and 8 months, but (PW) classified as silt with low plasticity (ML) at effect periods 12 and 16 months, based on the impact of industrial waste water, as per the unified classification system (USCS).
14. According to the effect of industrial paper wastewater (PW), and industrial dairy waste water (DW) classified as clay with high plasticity. On the other hand, industrial leather wastewater (LW) classified as (CH-MH) at effect periods 2 and 4 months and classified as (CH) at effect periods 6, 8, 12 and 16 months
15. For the soils (DW), (TW) and (PW) the (F.S) values were increase with the increase of contamination effect period, but for soil contaminated with Leather tanneries wastewater (LW)The free swell (F.S) values were decrease with the increase of contamination effect period.
16. The (F.S) results for the soil exposed to industrial wastewater from paper is more affected than soils exposed to other pollutants.
17. For all contaminated soil with the different industrial waste water the (GS) values were decrease with the increase of contamination effect period. But soil exposed to industrial wastewater from dairy (DW) is more affected than soils exposed to other pollutants.
18. Optimum moisture content (OMC %) values increase of contamination effect period for all contaminated soils (DW), (TW), (LW) and (PW)
19. For all contaminated soil with the different industrial waste water the maximum dry density (γdmax) values decrease with the increase of contamination effect period. But soil exposed to industrial wastewater from paper (PW) was the most affected.
20. The presence of industrial wastewater can lead to an increase in certain chemical oxides. But soil exposed to industrial wastewater from paper (PW) was the most affected. It includes a high percentage of Aluminum oxide (Al_2O_3), Iron oxide (Fe_2O_3), and Titanium oxide (TiO_2), in soil sample.
21. Some chemical oxides in soil samples are decreased due to the contamination by paper industrial wastewater it contains the lowest percentage of Silicon oxide (SiO_2), in soil sample, and some oxides are slightly decreased or increased. The above results of chemical oxides analysis agreed with the previous study by El-Kasaby, A., Easa, A.F (2023) and El-Kasaby, A., Easa, E.M (2023).
22. For the natural sample, the percentages of quartz, calcite, kaolinite, albite, and montmorillonite are 8.8%, 6.8%, 20.8%, 32.6 and 31%, respectively. While these components changed with the addition of textile wastewater (TW). Therefore, the Quartz, Calcite, Kaolinite (K), Ellite (I) and montmorillonite percentage are changed to 8.67%, 5.8%, 23.4%, 39.25%, and 22.88%, respectively. On the other hand, the components of control soil changed with the addition of dairy wastewater (DW). Therefore, the Quartz, Calcite, Kaolinite (K), albite (I) and montmorillonite percentage are changed to 9.38%, 5.5%, 22.85%, 38.77 and 23.5, respectively.
23. For the soil contaminated with leather wastewater (LW), the percentages of quartz, calcite, kaolinite, albite, and montmorillonite are 10.4%, 5.9%, 24.2%, 39.8 and 20%, respectively. While these components changed with the addition of paper wastewater (PW). Therefore, the Quartz, Calcite, Kaolinite (K), Ellite (I) and montmorillonite percentage are changed to 9.7%, 5.2%, 23.3%, 38.8%, and 23%, respectively. These results matched with the chemical composition of samples analyzed with XRF test.
24. The microstructure of the examined soils shows that, in comparison to the natural samples, the industrial wastewater increased the morphology's porosity and looseness.
25. The engineering qualities of soil, particularly free swelling, are severely reduced by effluent from dairy, textile and paper industries. Additionally, it is possible that the mineral particles would disintegrate, resulting in a loss of soil density. This loss of soil density can be identified as a significant Factor in the differences in soil parameters that were tested using SEM techniques.

REFERENCES

[1] Muhammad Irfan, Yulong Chen, Muhammad Ali, Muhammad Abrar, Ahmed Qadri and Osama Bhutta, (2018). Geotechnical properties of effluent - contaminated cohesive soils and their Stabilization using industrial by-products, Process Issue 6, No.203, pp 1-21

[2] Mitchell, J. (1993). Fundamentals of Soil Behavior; Wiley: New York, NY, USA.

[3] Gratchev, I.B.; Sassa, K. (2009). Cyclic behavior of fine-grained soils at different pH values. J. Geotech. Geoenviron. Eng. 135, 271–279.

[4] Terzaghi, K.; Peck, R.; Mesri, G. (1984). Soil Mechanics in Engineering Practice; John Wiley & Sons: New York, NY, USA.

[5] Sridharan, A.; Nagaraj, H. (2005). Plastic limit and compaction characteristics of fine-grained soils Proc. Inst. Civ. Eng. Ground Improv. 9, 17–22.

[6] Stalin, V.K.; Muthukumaran, K.; Kartikeyan, A. (2010) Effect of Liquid waste on the index and engineering behaviour of soils. In Proceedings of the Indian Geotechnical Conference: IGC-2000:
[7] The millennium conference, Mumbai, Indian, 13–15; pp. 229–230.
[8] El-Kasaby, E.A. (1978). "Foundation on Swelling Clay", Master Science Thesis, Department of Civil Engineering, University of Assuit, Egypt, 166 pp.
[9] Easa, AA and El-darder, M.E. (2002). "In-Situ Investigation of Mineralogical and Chemical Properties of Clayey Soil Contaminated with Wastewater", Engineering research journal, Helwan University. Vol. 84, pp. 150-161.
[10] El-Kasaby, A., Easa, A.A. Essa, A.F. (2023). International journal of advanced engineering, management and since, 75-91.
[11] ASTM D4318-17e1; (2017). Standard Test Methods for Liquid Limit, Plastic Limit, and Plasticity Index of Soils. ASTM International: West Conshohocken, PA, USA.
[12] El-Kasaby, A., Easa, E.M. Essa, E.M. (2023). International journal of advanced engineering, management and since, 39-54.
[13] AASHTO T90; (2020). Standard Method of Test for Determining the Plastic Limit and Plasticity Index of Soils. American Association of State Highway and Transportation Officials (AASHTO): Washington, DC, USA.
[14] Abd El-Latief, M. A., Ashour, M. B., & El-Tahrany, A. C. (2015). Strengthening of the permeability of sandy soil by different grouting materials for seepage reduction.
[15] BS EN ISO 17892-12:2018+A2 (2022). Geotechnical Investigation and Testing. Laboratory Testing of Soil. Part 12: Determination of Liquid and Plastic Limits. British Standards Institution: London, UK.
[16] Barnes, G.E. (2013). The Plastic Limit and Workability of Soils. Ph.D. Thesis, University of Manchester, Manchester, UK.
[17] Easa, A., & Abou-Rayan, A. (2010). Domestic wastewater effect on the pollution of the groundwater in rural areas in Egypt. aquatic, 3(4), 5.
[18] Casagrande, A. (1947). Classification and identification of soils. Proc. Am. Soc. Civ. Eng. 73, 783–810.
[19] O'Kelly, B.C. (2021). Review of recent developments and understanding of Atterberg limits determinations. Geotechnics, 1, 59–75.
[20] El-Kasaby, E. A., Eissa, E. A., Ab-Elmeged, M. F., & Abo-Shark, A. A. (2019). Coefficient of Consolidation and Volume Change for 3-D Consolidation. European Journal of Engineering and Technology Research, 4(5), 126-131.
[21] Wang, X. H., Zhang, Y., & Huang, C. H. (2014). Experimental study on the treatment of sewage by soil. Applied Mechanics and Materials, 464, 179-183.
[22] Cyrus S, Kumar TG, Abraham BM, Sridharan A, Jose BT (2010) Effect of industrial wastes on the physical and engineering properties of soils. Indian Geotechnical Conference GEOtrendz, pp 357–360
[23] El-Kasaby, E.A. and El-Saadany, M.M. (1993):" Soil investigations report of old mosques", El-Monofya state. Arab Engineering Consultants, Banha.
[24] El-Kasaby, E.A. and El-Saadany, M.M. (1993):" Effect of circumstances surrounding foundations on safety of constructions", 5th Arab Conf. on Stru. Eng., Civil Eng. Dep., Al-Fateh Univ., Tripoli, Libya.
[25] Crawford, C.B. and burn, K.N. (1992):" Settlement studies on the mt. Sinai hospital" Eng. Journal of Canada, Ottawa, Vol. 345, No. 22.
[26] Roberts, M.H.; Roy, D.M. and Kumar (1990):" Failer of buildings foundations on clay", Proc. Asce, Vol. 217, PP. 853-859.
[27] Sherif, M.; Mashhowr, M. and shatter, M. (1986):" Influence of the chemical composition of pore fluid on consistency and compression characteristics of clay", Journal of Egyptian Society of Engineers, Vol. 25, No. 4, PP. 9-16
[28] El-Kasaby, E.A. and El-Saadany, M.M. and Easa, E.A. (1994):" Influence of waste water on physic chemical properties and mineralogy of fine- grained soils" Second Conference on Civil Engineer, Military Technical College, Cairo, Vol. II, PP. 123-132
[29] El-Kasaby, E.A. and El-Saadany, M.M. and Easa, E.A. (1995):" Influence of waste water on index properties of fine-grained soil" Frist Engineering Conference, Faculty of Eng. Mansoura Univ., Mansoura, Vol III., PP 329-337.
[30] Bayoumy, S.M. (1988): "Effect of pollutions on its engineering properties ". M.SC.D. Thesis (Civil Eng.) Zagazig Univ., Egypt.
[31] Kirov, B. (1989). Influence of Wastewater on Soil Deformation. Proc. of 12th ICSMFE-1989, Brazil, pp. 1881-1882.
[32] Srivastava, R.K., Singh, M., Singh, B. and Tiwari, R.P. (1992). Soil-Fluid (Fertilizer Plant Effluent) interaction behaviour. Indian Geotechnical Conference, Calcutta, India, pp. 501-504.
[33] Yaji, R. K., Gowda Ramakrishna and Jha, Sandeep (1996). Influence of contamination on the behaviour of shedi soil, IGC-1996, December 1-14, Madras, Volume 1, pp. 540-543.
[34] 32-Güllü, H., & Girisken, S. (2013). Performance of fine-grained soil treated with industrial wastewater sludge. Environmental earth sciences, 70, 777-788.